ABSTRACT

Title of dissertation: THE HUNT VARIANCE GAMMA PROCESS WITH APPLICATIONS TO OPTION PRICING

Bryant Angelos, Doctor of Philosophy, 2013

Dissertation directed by: Professor Dilip Madan
Department of Finance

In this dissertation we develop a spatially inhomogeneous Markov process as a model for financial asset prices. This model is called the Hunt variance gamma process. We define it via its infinitesimal generator and prove that this generator induces a unique measure on the space of cádlàg functions. We next describe a procedure to do computations with this model by finding a continuous-time Markov chain approximation. This approximation is used to calibrate the model to fit the S&P 500 futures option surface. Next we investigate specific characteristics of the process, showing how it differs from both Lévy and Sato processes. We conclude by using the calibrated model to answer questions about properties of the risk-neutral distribution of future stock prices. We observe a more accurate fit to the risk-neutral term structure of volatility, skewness, and kurtosis, and the presence of mean-reversion in conditional probabilities involving large jumps.

# THE HUNT VARIANCE GAMMA PROCESS WITH APPLICATIONS TO OPTION PRICING

by

Bryant Angelos

Dissertation submitted to the Faculty of the Graduate School of the
University of Maryland, College Park in partial fulfillment
of the requirements for the degree of
Doctor of Philosophy
2013

Advisory Committee:
Professor Dilip B. Madan, Chair/Advisor
Professor Radu V. Balan, Co-Advisor
Professor Frank B. Alt
Professor John J. Benedetto
Professor Kasso Okoudjou

# Dedication

There is only one person to whom I can dedicate this thesis. And though she will probably never read more than a page of it, I couldn't have done it without her. Mary, thanks for everything. I love you.

# Acknowledgments

There are so many people who have contributed either directly or indirectly to this dissertation. It is impossible for me to acknowledge everyone who has helped me in some manner during my time at the University of Maryland.

Nevertheless, I would be negligent if I didn't at least make an effort to mention those who have contributed so much. To start, I have to mention my adviser, Dr. Dilip Madan. His enthusiasm and expertise piqued my interest in mathematical finance initially. As I learned more, I realized just how knowledgeable he was. But what impressed me most was his willingness to share that knowledge with his students in seminars and private conversations. Without his ideas, suggestions, and recommendations, I never would have reached this point.

I would also like to acknowledge the members of my committee for their work in reviewing and improving my work. Dr. Balan, Dr. Benedetto, Dr. Okoudjou, and Dr. Alt, thank you for taking time to help me. During the last few years, Dr. Balan has been especially kind in assisting me with a number of administrative details, for which I thank him.

Along these lines, I am grateful to the entire Norbert Wiener Center for allowing me to attend conferences, classes, and seminars throughout my time in Maryland. It is fitting that I will defend my dissertation during its seminar, and it is a privilege to call myself a friend of the NWC.

My friends and colleagues at the University have been a constant source of ideas, entertainment, and sometimes even distractions during my last four years.

I don't think I ever would have made it through qualifying exams without their support, and I surely wouldn't have been able to endure the ups and downs of research without their companionship. Travis, Tim, Alex, Mark, Richard, and Josh, thank you for your friendship over the years. I will miss our conversations after I leave the University.

Many people have assisted in less direct ways to this dissertation. These include teachers in both high school and college, and especially Jeff Humpherys from Brigham Young University. I should also mention friends from outside the University, who were at least willing to feign interest in my research long enough to appease me. Thanks also to Jim Tressel, Luke Fickell, and Urban Myer for their hard work on my behalf throughout the year, but especially during the fall.

Finally, I thank my family. Mom and Dad, thanks for your unwavering support and encouragement over the years. I still remember where it all started, doing refrigerator math problems and counting ducks as a child. To my brothers and sister-in-law (soon to be plural), I know you guys are always there for me. This is an achievement for all of us. I hope to put a copy of this dissertation in the library of the lake house, if it ever gets built. Lastly, thanks to the entire Tschaggeny family for your love and encouragement, and especially for allowing me to drag Mary 2000 miles away to Maryland. Families are forever, and I am grateful to be a part of this one.

# Table of Contents

List of Figures vi

1 Introduction 1
1.1 Mathematical Models in Finance . . . 1
1.1.1 Continuous Models . . . 1
1.1.2 Lévy Processes . . . 5
1.1.3 Extensions of Lévy Processes . . . 10
1.2 Dissertation Subject . . . 14
1.3 Dissertation Organization . . . 15

2 Lévy Processes 18
2.1 Definition and Lévy-Khintchine Theorem . . . 18
2.2 Examples . . . 21
2.3 Poisson Random Measures . . . 22
2.4 The Lévy Measure . . . 25
2.4.1 Finite Measure . . . 28
2.4.2 Paths of Finite Variation . . . 28
2.4.3 Paths of Infinite Variation . . . 30

3 The Hunt Variance Gamma Process 33
3.1 The Variance Gamma Process . . . 33
3.2 Definition of the Hunt Variance Gamma Process . . . 37
3.3 Existence and Uniqueness . . . 41

4 Computation Using the Hunt Variance Gamma Process 50
4.1 Markov Chain Approximations . . . 50
4.2 Convergence and Error Estimates . . . 57
4.3 Calibration . . . 61

5 Characteristics and Applications of the Hunt Variance Gamma Process 71
5.1 Relation to Lévy and Sato Processes . . . 71
5.1.1 Time Evolution of Moments . . . 72
5.1.2 Non-Infinite Divisibility of Marginal Distributions . . . 74
5.2 Term Structure of Marginal Distributions . . . 85
5.3 Mean Reversion in Conditional Jump Probabilities . . . 90
5.4 Conclusions and Further Work . . . 94

Bibliography 96

# List of Figures


1.1 The volatility surface . . . . . 4
1.2 Lévy process calibration for options from one expiration date . . . . . 9
1.3 Common stochastic process used in finance . . . . . 14
1.4 Comparison of Hunt VG process to other models . . . . . 16

2.1 A compound poisson process with associated random measure . . . . 26

4.1 A non-uniform discretization of the real line . . . . . 54
4.2 Error convergence of a Hunt VG process . . . . . 62
4.3 Fit statistics for a Hunt VG process . . . . . 66
4.4 Fit statistics for a variance gamma process . . . . . 67
4.5 A Hunt VG process fit to market data . . . . . 69
4.6 A variance gamma process fit to market data . . . . . 70

5.1 Skewness in a Hunt VG process . . . . . 75
5.2 Excess kurtosis in a Hunt VG process . . . . . 76
5.3 Fourier inversion of a Hunt VG distribution . . . . . 81
5.4 Fourier inversion of a variance gamma distribution . . . . . 82
5.5 Effect of convolution on Lévy measure . . . . . 84
5.6 Market and model term structure of moments . . . . . 88
5.7 Term structure of moment fit . . . . . 89
5.8 Jump probabilities conditional on large moves . . . . . 92

# Chapter 1

# Introduction

## 1.1 Mathematical Models in Finance

Stochastic processes are at the core of asset price models in finance. These processes can be classified into two broad categories based on their sample paths: the continuous processes and the discontinuous processes. In the following section, we will describe the evolution of stochastic processes used in finance, highlighting key differences between them. We will especially focus on characteristics of these processes which are important for asset price models.

### 1.1.1 Continuous Models

The earliest person credited with using advanced mathematics to model the value of a financial asset is Louis Bachelier in his 1900 thesis, [1] (see [2] for an English translation). In this paper, Bachelier used Brownian motion as the source of uncertainty in the model and assumed that stock prices $S_t$ were given by

$$S_t = S_0 + \sigma W_t,$$

where $W_t$ is a Brownian motion. Brownian motion continues to be one of the fundamental building blocks in financial modeling and option pricing in general.

One obvious drawback to Bachelier's model is that asset prices can (and almost

surely will) go negative in time. In a world of limited-liability companies, this is inappropriate. Subsequent models correct this error.

The most well known and popular model in mathematical finance is the Black-Scholes model. In the Black-Scholes model, Bachelier's model is modified so that the log returns are normally distributed, instead of the price changes. In this model, the asset price at time $t$ is given by

$$S_t = S_0 e^{\mu t + \sigma W_t}, \tag{1.1}$$

where once again $W_t$ is a Brownian motion.

This model was published by Black and Scholes in [3] and Merton in [4]. In these papers, Black, Scholes, and Merton develop several fundamental ideas, the most important being a method of continuous trading by which an option payoff can be perfectly replicated. This technique, known as delta-hedging, is still used today by practitioners all over the world (see [5]). Merton and Scholes won the Nobel Prize in Economics for this work in 1997 (Black had passed away at the time).

Under this model, the price of a European call option $C$ with strike $K$ and expiration time $T$ is given by the formula

$$C = S_0 N(d_1) - K e^{-rT} N(d_2),$$

where

$$\begin{aligned} d_1 &= \frac{\log(\frac{S_0}{K}) + (r + \frac{\sigma^2}{2})T}{\sigma\sqrt{T}} \\ d_2 &= \frac{\log(\frac{S_0}{K}) + (r - \frac{\sigma^2}{2})T}{\sigma\sqrt{T}}. \end{aligned}$$

Here $r$ is the risk-free interest rate, and the function $N$ is the cumulative distribution function of a standard normal distribution.

One can see that there are several inputs to the Black-Scholes formula. These include the current stock price $S_0$, the strike $K$, the time to expiration $T$, the current interest rate $r$, and the volatility of the process, $\sigma$. Of these, $S_0$, $K$, and $T$ are unambiguous, and $r$ can be reasonably inferred from interest rates such as LIBOR. However the volatility, $\sigma$, is unobservable. Because of this, traders will discuss option prices in terms of volatility, using the Black-Scholes formula as a map from volatility to price. Similarly, one can take option prices as an input, and invert the Black-Scholes formula to find what is known as the implied volatility. This is the volatility parameter $\sigma$ which, when used in the Black-Scholes formula, gives the observed option price.

It is assumed in the Black-Scholes formulation that volatility for a given stock is constant and unchanging. However, if we look at option prices from actual markets, we observe that the implied volatility is different as strike and maturity change. This is called the volatility smile or volatility surface. An example of the volatility surface can be seen in Figure 1.1. More information can be found in [6].

The curvature of the implied volatility surface increased markedly after the stock market crash of 1987 (see [7]), leading to efforts to find models which allowed for this phenomenon. There are two ways in which this has been done. The first way to do this is through a local volatility process. The second way is to allow jumps in prices.

The local volatility process was developed in the early 1990s and allows one

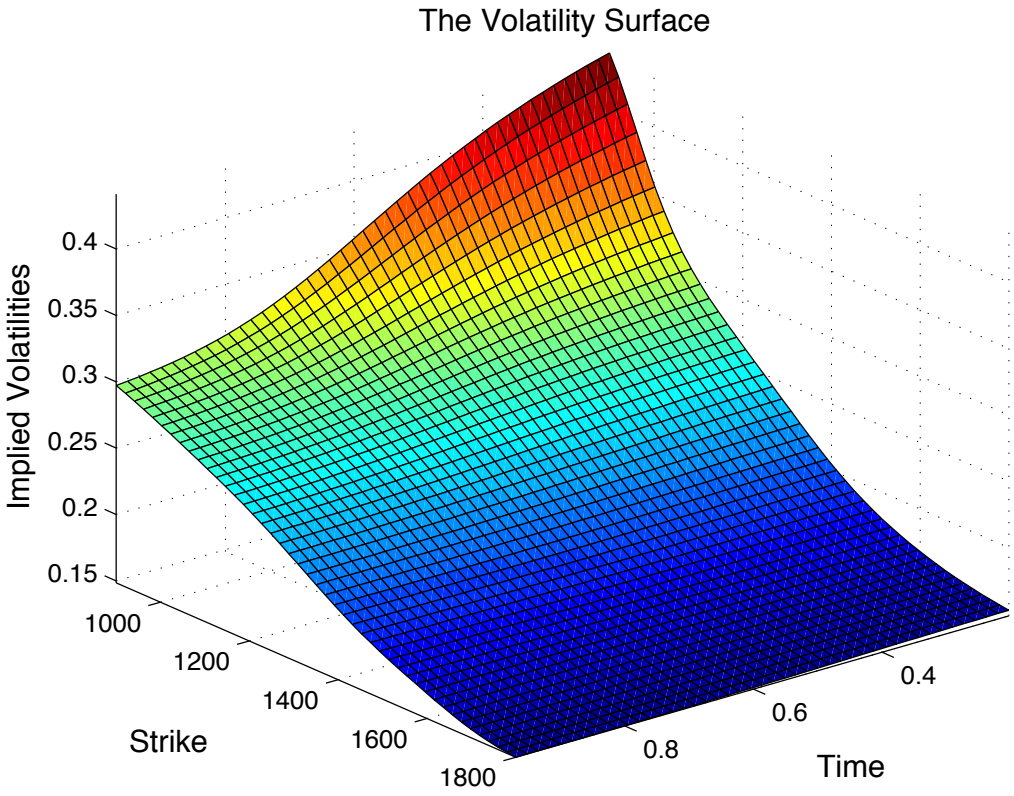


Figure 1.1: This figure shows the implied volatility surface for options on the S&P 500 index on January 3, 2012. One can observe that the implied volatility is higher for lower strikes and shorter expirations, a common feature of the volatility surface for equity options.

to fit the volatility surface exactly. This is accomplished by slightly modifying the Black-Scholes formula by making volatility a deterministic function of stock level and time. Here the model satisfies the SDE

$$\frac{dS_t}{S_t} = \mu\, dt + \sigma(t, S_t)\, dW_t.$$

In [8] and [9], Dupire, Derman, and Kani showed that if $\sigma$ satisfies certain conditions, this model will exactly replicate the option volatility surface. To denote this volatility, we let $C(K, T)$ represent the price of a call option with strike $K$ and expiration time $T$, data which is available from the market. They then showed that volatility $\sigma$ should satisfy

$$\frac{\partial C}{\partial T}(K,T) = \frac{1}{2}\sigma(K,T)K^2\frac{\partial^2 C}{\partial K^2}(K,T) - rK\frac{\partial C}{\partial K}(K,T).$$

Local volatility models successfully fit the option volatility surface, but they are not perfect. One issue is that these models assume that the stock price process is continuous, while even a glimpse at a stock chart will show that such an assumption is not warranted. Another issue is that, in theory, this model requires the parameterization of an entire function from $\mathbb{R}^2$ to $\mathbb{R}$, an infinite dimensional problem. In practice, there will be one parameter for every option trading in the market, which can number in the hundreds. This leads to difficulties in understanding and adapting this model for other assets.

### 1.1.2 Lévy Processes

The second major branch from the Black-Scholes model was the introduction of jumps in the asset price. Robert Merton was the first person to drop the requirement

that asset prices move continuously, see [10]. Shortly after the introduction of the Black-Scholes model, he wrote a paper in which he uses a Poisson process $N_t$ to model the arrival of jumps, where jump sizes are i.i.d. random variables $Y_i$. In his model, the stock price is given by

$$S_t = S_0 e^{\mu t + \sigma W_t + \sum_{i=1}^{N_t} Y_i}.$$

One consequence of this model is that we can no longer dynamically hedge options payoffs, as we could using the Black-Scholes model. This makes the problem of asset pricing more difficult, because options can no longer be priced using only the assumption of no arbitrage. However, it is more appealing on a practical level because continuous trading is impossible and would be prohibitively expensive even if it were. This leads to many interesting questions about hedging, which is an active area of research. For an overview, see [11].

We should also note that empirical evidence exists showing the existence of jumps in the risk-neutral price process. In a continuous model, the price of an out of the money option with short maturity should be near 0. In contrast, a jump process can jump into the money more readily, and so higher prices are expected. By observing the rate at which the price of an out of the money option approaches 0, we can see evidence for the existence of jumps in the price process. This was done in [12].

Since Merton's initial paper, a great deal of research has been done to explore the use of discontinuous processes. Processes which have independent and stationary increments are the simplest of this type and are called Lévy processes. We will

discuss Lévy processes in more detail in Chapter 2, but we discuss a few key aspects of the theory here.

A major theorem about Lévy processes is the Lévy- Khintchine theorem, which is given in more detail in equation (2.1.4). This theorem describes the characteristic function of any Lévy process in terms of three parameters: a drift term, a Brownian term, and a measure called the Lévy measure. The drift and Brownian term describe the continuous motion of the process, while the Lévy measure describes the jump structure. Most Lévy processes used in finance are described in terms of these three parameters.

One significant advancement which allowed Lévy processes to flourish was the discovery of Fourier transform methods for option pricing. Recall that the characteristic function of a process $X_t$ is given by

$$\Psi(u) = \mathbb{E}[e^{iuX_t}],$$

which is the Fourier transform of the probability measure associated with $X_t$. The characteristic function of a Lévy process is readily accessible because of the Lévy-Khintchine theorem, and so the function $\Psi$ is easily calculated. In 1999, Carr and Madan showed how to value options when the characteristic equation of the log-price process is known (see [13]). Lewis developed a similar method in [14]. These methods use the fast Fourier transform to compute option prices, which allows for extremely efficient computation. A fast and accurate pricing method is useful because many times option pricing formulas are used in calibration, which require the pricing algorithm to be called a large number of times. This theory is summarized in [15].

A simple method to construct a Lévy process is to take a continuous Brownian motion and time change it using an increasing process. This was the method used by Madan et al. in constructing the variance gamma model, which is a Brownian motion time-changed by an increasing gamma process (see [16], [17], and [18]). Other processes constructed in this manner are the normal inverse Gaussian (NIG) model ([19]) and the generalized hyperbolic (GH) model ([20]).

Another method to construct a Lévy process is by specifying the Lévy measure directly. This allows one to develop Lévy processes with specific features of interest in the model, for example finite versus infinite jump activity, and finite or infinite variation. Examples of Lévy processes of this type are the CGMY model in [21], the KoBoL model in [22], and the Meixner process in [23]. Another example of this type is the $\beta$-family of Lévy processes, described by Kuznetsov in [24] and [25] for use in pricing barrier options. A fine source describing these and other Lévy processes is [26].

Lévy processes and jump models in general do a good job of fitting the volatility smile for a single maturity, but are not as successful when calibrated to multiple maturities. Figure 1.2 shows the fit of a simple Lévy process to options with the same expiration date. One reason Lévy processes can fit the option surface is that these processes are able to incorporate skewness and kurtosis into the marginal distribution of stock returns. In contrast, Brownian motion has zero skewness and excess kurtosis, which is one possible explanation for the volatility smile, see [27].

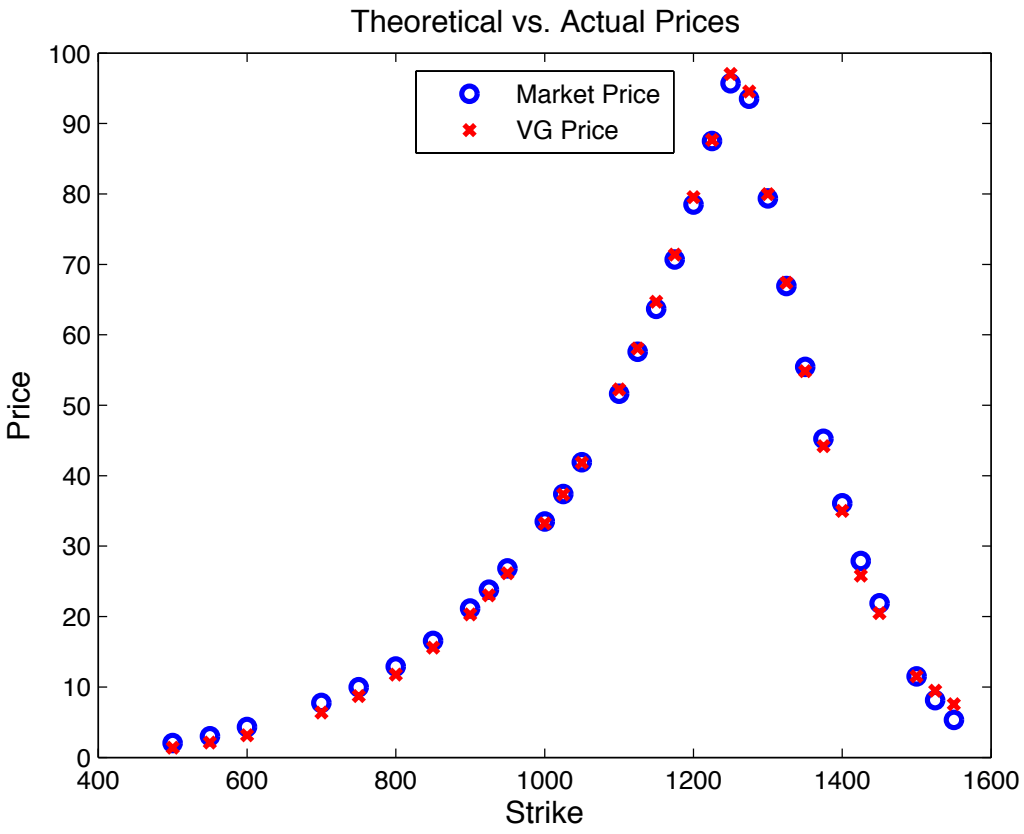


Figure 1.2: This figure shows the market and model prices for options on the S&P 500 index on January 3, 2012. The model is a variance gamma Lévy process, one of the first Lévy processes used in financial modeling.

### 1.1.3 Extensions of Lévy Processes

One critique of Lévy processes is that the skewness and kurtosis of the Lévy process scale deterministically in time. In [28], it was noted that skewness decays according to $1/\sqrt{t}$, while kurtosis decays according to $1/t$. This is a feature of the linear nature of the evolution of the characteristic exponent in time. Market data can be used to show that market option prices have risk neutral distributions which do not evolve in this manner, see [29] and [30]. All Lévy processes have this characteristic decay, so no amount of modification will produce a Lévy process which fits the market evolution of marginal distributions.

This observation lead to the use of additive processes in finance. An additive process is similar to a Lévy process, except that the condition of stationary increments is dropped. This means that for a sequence of times $t_0 < t_1 < \ldots < t_n$, the random variables $X_{t_0}$, $X_{t_1} - X_{t_0}$, $\ldots$, $X_{t_n} - X_{t_{n-1}}$ are independent, but not necessarily identically distributed. These processes are space homogeneous Markov processes which are not time homogeneous.

The major class of additive processes used in finance are the Sato processes, developed in [31]. These processes satisfy the property that

$$X_t = t^\gamma X,$$

where $X$ is a self decomposable random variable and the equality is in distribution.

The characteristic equation of these processes has a convenient form. If the characteristic equation of $X$ can be written as

$$\mathbb{E}[e^{iuX}] = e^{\psi(u)},$$

then the characteristic equation of the process $X_t$ is given by

$$\mathbb{E}[e^{iuX_t}] = e^{\psi(ut^\gamma)}. \tag{1.2}$$

This allows one to use the Fourier option pricing methods discussed previously to quickly price options and calibrate process of this type.

Another extension of the Lévy process are the local Lévy models. These processes are both time and space inhomogeneous and are an extension of the local volatility models described previously. To form a process of this type, the compensator of a jump process (the Lévy measure, which we will denote $\Pi(dx)$) is multiplied by a speed function, $a(S_t, t)$. This function plays a role similar to the volatility function, $\sigma(S_t, t)$, in a local volatility model. In [32], it is shown that the speed function should satisfy the equation

$$C_T + rKC_K = \int_0^\infty C_Y Y Y a(Y,T)\psi_e\left(\log(\frac{K}{Y})\right) dY, \tag{1.3}$$

where $C$, $K$, and $r$ have the usual meaning. In this equation, $\psi_e$ is the exponential double tail of the Lévy measure, which is given by

$$\psi_e(z) = \begin{cases} \int_{-\infty}^{z} dx\, e^x \int_{-\infty}^{x} \Pi(u)\, du & \text{if } z < 0 \\ \int_{z}^{\infty} dx\, e^x \int_{x}^{\infty} \Pi(u)\, du & \text{if } z > 0 \end{cases}.$$

These models requires the parameterization of the entire function $a : \mathbb{R}^2 \to \mathbb{R}$. Like the local volatility models, this model requires an infinite number of parameters, which in practice reduces to one parameter for every option trading in the market.

The final common extensions are the stochastic volatility models, both with and without jumps. In these models, the asset price $S_t$ is no longer a Markov process,

but if you include one or more dimensions, the resulting system is Markovian. In diffusion models of this type, it is usually assumed that

$$\frac{dS_t}{S_t} = \mu\, dt + \sigma_t\, dW_t,$$

where $\sigma_t$ is a random process called the volatility process.

To model the volatility, two important factors are usually considered. First, volatility must be positive; and second, volatility is usually believed to be mean-reverting. To accomplish this, we set $\sigma_t = f(y_t)$, where $f$ is a positive function and $y_t$ is a mean reverting process. We note that it is a simple matter to introduce correlation between the volatility and the asset returns, a desirable feature which is manifest in markets and is sometimes referred to as volatility clustering (see [33]).

Several models have been proposed for the underlying volatility process $y_t$. These include modeling $y_t$ as geometric Brownian motion in the Hull–White model in [34] and as a Gaussian Ornstein-Uhlenbeck process in [35].

However, the most influential model is the Heston model in [36]. This model satisfies the requirement that volatility be positive and mean reverting by setting the function $f(y_t) = \sqrt{y_t}$. We then allow $y_t$ to follow what has come to be known as a Cox-Ingersol-Ross (CIR) process, in which $y_t$ satisfies the stochastic differential equation

$$dy_t = \kappa(\eta - y_t)\, dt + v\sqrt{y_t}\, dW_t^{(2)}.$$

Here $\eta$ is the long-run average value of $y_t$, while $\kappa$ is the rate of mean reversion. $W_t^{(2)}$ is a second Brownian motion that can be made to correlate to the Brownian motion in the asset price process. This process is sometimes also called the square

root process, because the square root in the last term of this equation forces $y_t$ to remain positive. This model has been extended to allow the parameters $\eta$ and $\kappa$ to be time dependent, for example in [37].

It is also the case that stochastic volatility models can be designed to incorporate discontinuities. These stochastic jump models share many of the same characteristics as their continuous relatives. The simplest and best known model of this type is the Bates model, see [38]. This model differs from the Heston model by adding a compound Poisson process $Z_t$ to the asset price, so that

$$\frac{dS_t}{S_t} = \mu\, dt + \sigma_t\, dW_t + dZ_t.$$

The addition of this jump component allows one to fit the volatility surface at short time periods using the jump parameters, while adjusting the correlation between asset price and volatility level to introduce a smile at longer maturities.

Of course, more complicated stochastic volatility models can be developed by allowing the volatility to develop in a discontinuous manner. Barndorff-Nielen and Shephard have developed a model in [39] in which the uncertainty driving the volatility is a Lévy process.

Stochastic volatility models are currently the state-of-the-art in financial modeling. However, there are shortcomings with these models as with all of the others. It can be shown that if the stock price follows a 1-dimensional Markovian process, than the option surface is arbitrage free (see [40]). Stochastic volatility models are 2-dimensional Markov processes, and so there is unnecessary dimensionality in these models.

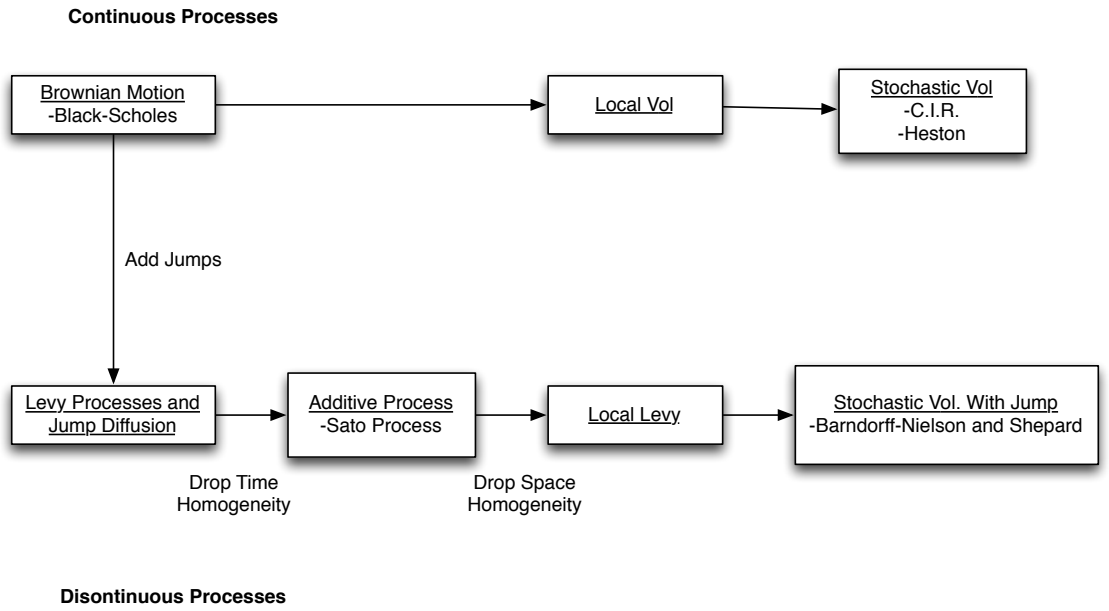


Figure 1.3: This figure gives an overview of common stochastic processes used in finance. Continuous processes are found on the top line, while discontinuous processes form the bottom line. The complexity of the process also increases from left to right.

For further information on stochastic processes used in finance, we refer the reader to the excellent summary in [41]. Figure 1.3 also shows a convenient way to observe the different types of models currently in use.

## 1.2 Dissertation Subject

In this dissertation, we will define a stochastic process that has previously not been used in financial modeling. This process, which we call the Hunt variance gamma process, is a one dimensional Markov process which is spatially inhomogeneous and temporally homogeneous. Its closest analog is the Sato process, which has the opposite characteristic of being spatially homogeneous while being time-

inhomogeneous. Figure 1.4 describes the mathematical relationship between Lévy processes, the Hunt variance gamma process, Sato processes, and local Lévy processes in graphic form.

As a model for pricing financial instruments, the Hunt variance gamma process combines several of the nice features of these related processes. First of all, it can be described in only a few parameters, as opposed to the local Lévy models which require describing the entire speed function $a : \mathbb{R}^2 \to \mathbb{R}$ (see equation **??**LocalLevySpecificationForAEqn)). Unlike a regular Lévy process, the Hunt variance gamma process can, after calibration, effectively price options at several maturities simultaneously. Finally, unlike Sato processes, the Hunt variance gamma process can more accurately describe the term structure of moments, found in the market. We explore each of these features in more detail in other parts of this dissertation.

## 1.3 Dissertation Organization

The remainder of this dissertation is organized in the following way. Chapter 2 gives an overview of Lévy processes, with definitions, examples, and key theorems. Lévy processes are the base from which we develop the Hunt variance gamma process, so we discuss them in some depth. We define the Hunt variance gamma process in Chapter 3, and prove some existence and uniqueness results as well. In Chapter 4, we describe a method to do calculations using the Hunt variance gamma process, and use it to calibrate several Hunt variance gamma processes to market prices over

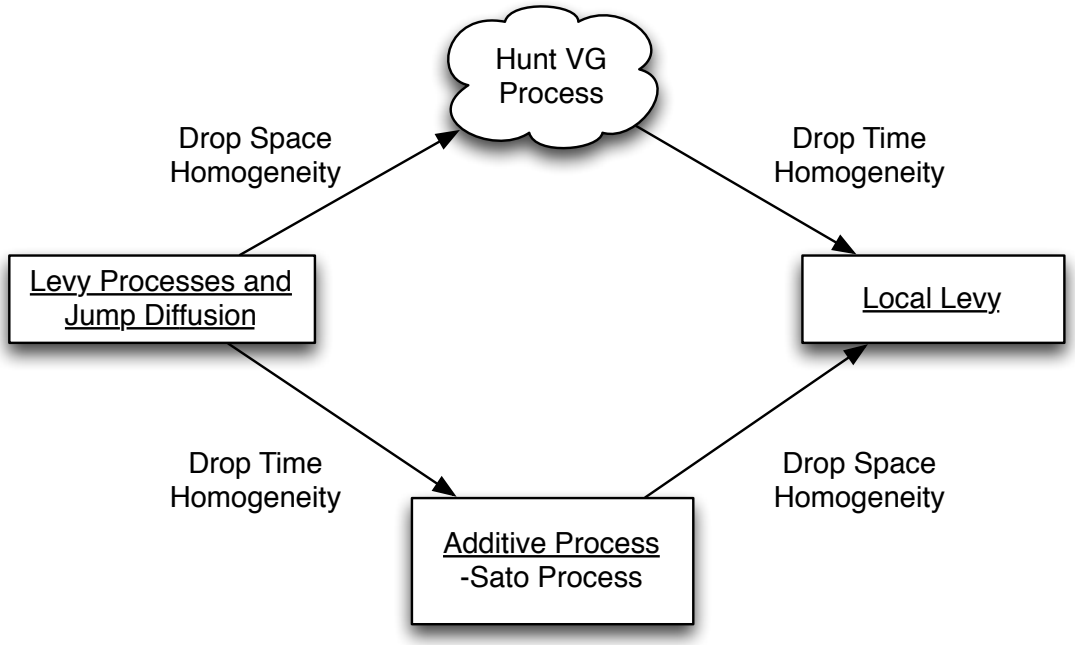


Figure 1.4: This figure shows how the Hunt variance gamma process relates to other common financial models. The Hunt variance gamma process can be obtained from a Lévy process by dropping the requirement of spatial homogeneity. If time-homogeneity is also not required, this process can be classified as a local Lévy process.

five years. This method is based on recent work which demonstrates a method to approximate one-dimensional Markov processes using Markov chains. In Chapter 5, we investigate several characteristics and applications of the Hunt variance gamma process, using the calibrations from Chapter 4.

# Chapter 2

# Lévy Processes

In this chapter, we describe the general theory of Lévy processes. We will review the definition together with some of the fundamental theorems of these processes. We also give some examples of specific Lévy processes to gain a more intuitive understanding of their characteristics.

Lévy processes serve as a point of departure for the Hunt variance gamma process which we describe in later chapters of this dissertation, so this is a natural starting point.

## 2.1 Definition and Lévy-Khintchine Theorem

Lévy processes are a class of stochastic processes which have become extremely popular in recent years. They are commonly used to model financial instruments. In this section, we define Lévy processes and explain some of their common features. For a more thorough treatment of the subject, the reader is invited to look at classic textbooks on the subject, such as [42], [43], or [44].

**Definition 2.1.1.** *A stochastic process $X_t$ on the probability space $(\Omega, \mathscr{F}, \mathbb{P})$ is called a Lévy process if:*

1. *$X_0 = 0$ almost surely*

2. *For any $n \geq 1$ and for $0 \leq t_0 < \cdots < t_n$ we have that the random variables*

$X_{t_0}, X_{t_1} - X_{t_0}, \cdots, X_{t_n} - X_{t_{n-1}}$ *are independent.*

3. $X_t$ *has stationary increments* ($X_t - X_s$ *has the same distribution as* $X_{t-s}$)

4. $X_t$ *is cádlàg, meaning paths are right continuous with left limits almost surely*

5. $X_t$ *is stochastically continuous, meaning that for every* $t \geq 0$ *and* $\epsilon > 0$,

$$\lim_{s \to t} \mathbb{P}(|X_s - X_t| > \epsilon] = 0$$

Observe that any Lévy process which is continuous is a Brownian motion, so Brownian motion is a type of Lévy process.

**Definition 2.1.2.** *A probability measure* $\mathbb{P}$ *on* $\mathbb{R}$ *is called infinitely divisible if for any positive integer* $n$*, there exists* $n$ *independent and identically distributed random variables* $X_1, \cdots, X_n$ *such that the distribution of* $X_1 + \cdots + X_n$ *is equal to that of* $\mathbb{P}$.

If $X_t$ is a Lévy process, one can write

$$X_t = (X_{t/n} - X_0) + \cdots + (X_t - X_{(n-1)t/n}) \tag{2.1}$$

for any positive integer $n$, showing that the distribution of a Lévy process is infinitely divisible. It is also the case that one can construct a Lévy process from any infinitely divisible distribution.

The most important theorem about infinitely divisible distributions is the Lévy-Khintchine formula.

**Theorem 2.1.3** (Lévy-Khintchine)**.** *For any infinitely divisible measure $\mathbb{P}$, its characteristic function can be written as*

$$\int_{\mathbb{R}} e^{iux}\mathbb{P}(dx) = e^{\psi(u)},$$

*where*

$$\psi(u) = i\mu u - \frac{1}{2}\sigma^2 u^2 + \int_{\mathbb{R}} \left(e^{iux} - 1 - iux\mathbf{1}_{\{|x|<1\}}\right)\Pi(dx) \tag{2.2}$$

*and* $\int(1 \wedge x^2)\Pi(dx) < \infty$.

*Similarly, given* $(\mu, \sigma^2, \Pi(dx))$ *such that* $\int(1 \wedge x^2)\Pi(dx) < \infty$*, there exists an infinitely divisible probability measure* $\mathbb{P}$ *with characteristic exponent given by equation (2.2).*

As Lévy processes and infinitely divisible measures are in one-to-one correspondence, one can rewrite this theorem as it applies to Lévy processes. One should note that because of the decomposition given in equation (2.1), the characteristic exponent of $X_t$ can be written in terms of the characteristic exponent of $X_1$. The following, more common, form of the Lévy-Khintchine theorem illustrates this.

**Theorem 2.1.4** (Lévy-Khintchine)**.** *The characteristic function of any Lévy process $X_t$ can be written as*

$$\mathbb{E}[e^{iuX_t}] = e^{t\psi(u)},$$

*where*

$$\psi(u) = i\mu u - \frac{1}{2}\sigma^2 u^2 + \int_{\mathbb{R}} \left(e^{iux} - 1 - iux\mathbf{1}_{\{|x|<1\}}\right)\Pi(dx) \tag{2.3}$$

*and* $\int(1 \wedge x^2)\Pi(dx) < \infty$*. Here* $\psi(u) = log(\mathbb{E}[e^{iuX_1}])$.

*Similarly, given* $(\mu, \sigma^2, \Pi(dx))$ *such that* $\int (1 \wedge x^2)\Pi(dx) < \infty$, *there exists a Lévy process with characteristic exponent given by equation (2.3).*

The function $\psi$ is called the characteristic exponent. The parameters $(\mu, \sigma^2, \Pi(dx))$ together are called the Lévy triplet of a Lévy process, and uniquely characterize it. The measure $\Pi(dx)$ is called the Lévy measure.

## 2.2 Examples

We will now give a few examples of the characteristic exponents of Lévy processes.

**Example 2.2.1.** *Let* $X_t$ *be a Brownian motion, with parameters* $(\mu, \sigma^2)$. *This means that* $X_t$ *is distributed normally with mean* $\mu t$ *and variance* $\sigma^2 t$. *One can integrate to see that*

$$\mathbb{E}[e^{iuX_t}] = e^{i\mu ut - \frac{1}{2}\sigma^2 u^2 t},$$

*and so*

$$\psi(u) = i\mu u - \frac{1}{2}\sigma^2 u^2.$$

*We see that the Lévy triplet is given by* $(\mu, \sigma^2, 0(dx))$.

**Example 2.2.2.** *A Poisson process is a one parameter Lévy process. If* $N_t$ *is a Poisson process with parameter* $\lambda$, *then it has measure* $\mathbb{P}$ *satisfying*

$$\mathbb{P}[N_t = k] = \frac{e^{-\lambda t}(\lambda t)^k}{k!}.$$

*To construct a compound Poisson process, we let* $N_t$ *be as shown, and define*

$X_t := \sum_{i=1}^{N_t} Y_i$, *where the random variables* $Y_i$ *are independent, identically distributed random variables having some law* $F$.

*Then once again, by first conditioning on* $N_t$ *and then summing we can find that*

$$\mathbb{E}[e^{iuX_t}] = e^{\lambda t \int_{\mathbb{R}}(e^{iux}-1)F(dx)}$$

*and so*

$$\psi(u) = \lambda \int_{\mathbb{R}} (e^{iux} - 1)F(dx).$$

*The Levy triplet is* $\mu = \lambda \int_{-1}^{1} xF(dx)$, $\sigma^2 = 0$, *and* $\Pi(dx) = \lambda F(dx)$.

These two examples provide a great deal of intuition about the meaning of the Lévy triplet. We see from Example 2.2.1 that the parameters $\mu$ and $\sigma^2$ correspond to the drift and variance of a brownian motion. We also observe in Example 2.2.2 that we can construct a variety of Lévy measures $\Pi$ by simply varying the intensity $\lambda$ and underlying law $F$ of a complex poisson process.

We will see in Section 2.4 that these two examples are the main building blocks for any Lévy process.

## 2.3 Poisson Random Measures

To better understand the jump structure of Lévy processes, we introduce the subject of Poisson random measures.

**Definition 2.3.1.** *Let* $(E, \mathscr{E})$ *be a measurable space, and let* $(\Omega, \mathscr{F}, \mathbb{P})$ *be a probability space. A random measure* $N$ *is a mapping* $N : \Omega \times \mathscr{E} \to \overline{\mathbb{R}}_+$ *which satisfies the following:*

1. *For each $A \in \mathscr{E}$, the mapping $\omega \to N(\omega, A)$ is a random variable*

2. *$\mathbb{P}$ almost surely, $A \to N(\omega, A)$ is a measure on $(E, \mathscr{E})$*

We are interested in counting measures, where the measure $N(\omega, \cdot)$ is atomic and every atom has weight one. In this case, $N$ maps into $\{0, 1, 2, \cdots\} \bigcup \{\infty\}$.

**Definition 2.3.2.** *Let $E = (\mathbb{R}/\{0\} \times [0, \infty])$ and $\mathscr{E}$ be the product topology. Let $\eta$ be a measure on $(E, \mathscr{E})$. A Poisson random measure is a random measure $N$ where the following conditions hold:*

1. *for disjoint sets $A_1, A_2, \cdots, A_n \in \mathscr{E}$, the random variables $N(\cdot, A_1), N(\cdot, A_2), \cdots N(\cdot, A_n)$ are independent,*

2. *for each $A \in \mathscr{E}$, the random variable $N(\cdot, A)$ follows a Poisson distribution with parameter $\eta(A)$. If $\eta(A) = 0$ then $N(\cdot, A) = 0$, and if $\eta(A) = \infty$, $N(\cdot, A) = \infty$.*

*The measure $\eta$ is called the intensity of $N$.*

Proof of the existence of Poison random measures can be found in [45] or [46]. When the meaning is clear, we will not denote the dependence of $N$ on $\Omega$, writing for example, $N(A)$ instead of $N(\cdot, A)$. As $E = (\mathbb{R}/\{0\} \times [0, \infty])$, we will usually represent a set in $E$ as $A \times B$ and the random measure of that set by $N(A, B)$ instead of $N(A \times B)$.

As $N$ is a measure almost surely, we can use the standard results in measure theory to integrate. These techniques can be found anywhere; we mention [47] and

[48] specifically. This allows us to consider integrals of the form

$$\int_0^T \int_{\mathbb{R}/\{0\}} f(x,t)N(dx,dt).$$

In the case of Poisson random measures, the support of $N$ is countable almost surely (see [43]), and so this integral can be written as

$$\sum_{(x_i,t_i)} f(x_i,t_i)$$

where $(x_i,t_i)$ are points where $N$ has support, counted without multiplicity.

With these definitions in hand, we introduce the major theorem of this section.

**Theorem 2.3.3.** *Let $N$ be a Poisson random measure with intensity $\eta$ on the measure space $(E,\mathscr{E})$. Let $f : E \to \mathbb{R}$.*

1. *The random variable*

$$X = \int_E f(x,t)N(dx,dt)$$

*is almost surely absolutely convergent if and only if*

$$\int_E (|f(x,t)| \wedge 1)\, \eta(dx,dt) < \infty \tag{2.4}$$

2. *If equation (2.4) holds, then the characteristic function of $X$ is given by*

$$\mathbb{E}[e^{iuX}] = \exp\left(\int_E (e^{iuf(x,t)} - 1)\eta(dx,dt)\right) \tag{2.5}$$

The proof of this result can be found in [45] or [49].

We now wish to relate this back to Example 2.2.2, demonstrating that a compound Poisson process can be written in terms of the integral of a Poisson random measure. Define an intensity measure $\eta$ on $\mathbb{R}/\{0\} \times [0,\infty]$ by $\eta = \lambda F \times \text{Leb}$, where

$\lambda > 0$, $F$ is a probability law, and Leb represents Lebesgue measure. Using $\eta$, we can construct a probability space and Poisson random measure $N$, and then define

$$X_t = \int_0^t \int_{\mathbb{R}/\{0\}} xN(ds, dx).$$

This integral will converge absolutely using Theorem 2.3.3 because

$$\int_0^t \int_{\mathbb{R}/\{0\}} (|x| \wedge 1)\lambda F(dx)ds < \infty.$$

Furthermore, its characteristic exponent is also given from Theorem 2.3.3, and is given by

$$\begin{aligned} \mathbb{E}[e^{iuX_t}] &= \exp\left(\int_0^t \int_{\mathbb{R}/\{0\}} (e^{iux} - 1)\lambda F(dx)ds)\right) \\ &= \exp\left(t\int_{\mathbb{R}/\{0\}} (e^{iux} - 1)\lambda F(dx)\right). \end{aligned}$$

This matches the characteristic exponent of a compound Poisson process given in equation (2.2.2), and so these two processes are equal in distribution.

A sample path of this process is given in Figure 4.1. Here $\lambda = 10$ and $F$ is a uniform measure on the set $[-2, 2]$. The support of the Poisson random measure $N$ is also marked, so one can see the size and times of the jumps associated with a Poisson random measure.

## 2.4 The Lévy Measure

We are now in position to describe the relationship between Lévy processes and Poisson Random measures. We can also describe some properties of the paths of Lévy processes based on their Lévy measures.

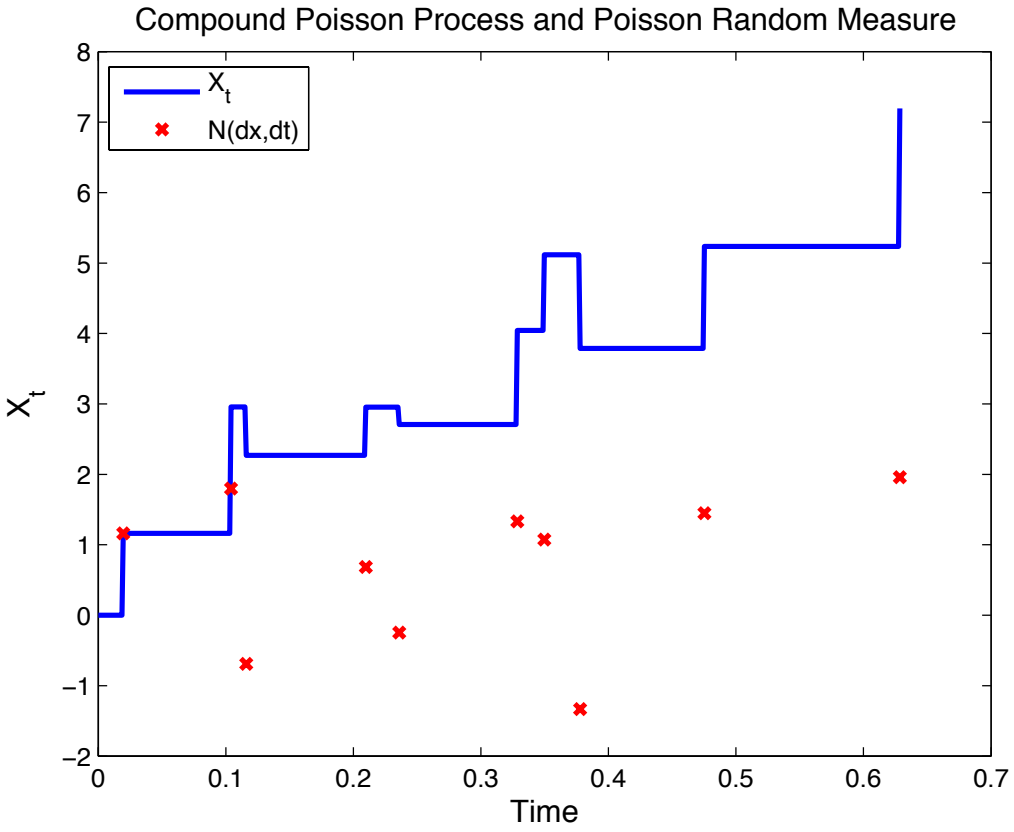


Figure 2.1: A sample path of $X_t = \int_0^t \int_{\mathbb{R}/\{0\}} xN(dx, ds)$, together with support of the Poisson random measure $N$. For this image, $N$ has generator given by $\lambda F \times \text{Leb}$ where $\lambda = 10$ and $F(A) = \frac{1}{4}\int_A \mathbb{1}_{[-2,2]}(s)dx$.

Suppose that a Lévy process $X_t$ has characteristic exponent given by

$$\psi(u) = i\mu u - \frac{1}{2}\sigma^2 u^2 + \int_{\mathbb{R}} \left(e^{iux} - 1 - iux\mathbf{1}_{\{|x|<1\}}\right) \Pi(dx).$$

From the Lévy-Khintchine theorem (Theorem 2.1.4), we know that this uniquely identifies a Lévy process.

The path properties of $X_t$ are intimately related to the Lévy measure $\Pi$. There are three cases to consider:

1. $\int_{\mathbb{R}/\{0\}} \Pi(dx) < \infty$
2. $\int_{\mathbb{R}/\{0\}} \Pi(dx) = \infty$ but $\int_{\mathbb{R}/\{0\}} (1 \wedge |x|)\Pi(dx) < \infty$
3. $\int_{\mathbb{R}/\{0\}} (1 \wedge |x|)\Pi(dx) = \infty$ but $\int_{\mathbb{R}/\{0\}} (1 \wedge x^2)\Pi(dx) < \infty$

Note that since a Lévy measure must satisfy $\int_{\mathbb{R}} /\{0\}(1 \wedge x^2)\Pi(dx) < \infty$, any Lévy process will fall into one of these three categories. The first category corresponds to compound Poisson processes, the second to processes of bounded variation, and the third to processes of unbounded variation. Each of these categories is explained below.

Before we continue, we make one note. If $\sigma > 0$, we can write $X_t = \sigma W_t + Y_t$, where $W_t$ is a standard Brownian motion and $Y_t$ is an independent Lévy process. $Y_t$ will then have Lévy triplet $(\mu, 0, \Pi)$. As Brownian motion has unbounded variation (see [50]), $X_t$ will always have unbounded variation if $\sigma > 0$. In the discussion to follow, we assume that $\sigma = 0$ so there is no Brownian component to the Lévy process.

### 2.4.1 Finite Measure

We first consider the case where $\Pi(\mathbb{R}/\{0\}) < \infty$. In this case, set $\lambda = \Pi(\mathbb{R}/\{0\})$, and define a measure $F$ on $\mathbb{R}$ such that $F(A) = \frac{\Pi(A)}{\lambda}$. Observe that $F(\mathbb{R}) = 1$, and so $F$ is a probability measure on $\mathbb{R}$.

Using these parameters, define a compound Poisson process as in example 2.2.2. We let $N_t$ be a Poisson process with parameter $\lambda$, and $Y_i$ a sequence of independent and identically distributed random variables with law $F$. Then we can write $X_t := \sum_{i=1}^{N_t} Y_i$. The characteristic function for this process is given in equation (2.2.2).

We showed in the previous section that such a process can be written in terms of a Poisson random process with intensity measure $\eta$ on $\mathbb{R}/\{0\} \times [0, \infty]$ given by $\eta(A, B) = \Pi(A)\text{Leb}(B)$. We can also apply Theorem 2.3.3 to the function $f(x) = 1$ to show that a Poisson process have a finite number of jumps by noting that $\int_{[\mathbb{R}/\{0\}]}(1)\Pi(dx) < \infty$. Thus Poisson processes have bounded variation.

### 2.4.2 Paths of Finite Variation

In this section we consider Lévy process with Lévy measures satisfying $\int_{\mathbb{R}/\{0\}} \Pi(dx) = \infty$ but $\int_{\mathbb{R}/\{0\}}(1 \wedge |x|)\Pi(dx) < \infty$. In this case, we cannot construct a compound Poisson process out of the Lévy measure. Instead, we turn directly to Poisson random measures to define our process. As before, we define a Poisson random measure $N$ by specifying its intensity $\eta$ on $\mathbb{R}/\{0\} \times [0, \infty]$ by $\eta = \Pi \times \text{Leb}$.

We define a Lévy process $X_t$ by

$$X_t = \int_0^t \int_{\mathbb{R}/\{0\}} xN(dx, ds). \tag{2.6}$$

We can once again appeal to Theorem 2.3.3 to prove that $X_t$ is defined almost surely, because

$$\int_0^t \int_{\mathbb{R}/\{0\}} (|x| \wedge 1)\Pi(dx)ds < \infty.$$

We can also use Theorem 2.3.3 part (ii) to compute that the characteristic function of this process is given by

$$\mathbb{E}[e^{iuX_t}] = \exp\left(t \int_{\mathbb{R}/\{0\}} (e^{iux} - 1)\Pi(dx)\right).$$

This characteristic exponent takes a slightly different form than that given in the Lévy Khintchine formula (Theorem 2.1.4). It can be made to match by computing $\int_{-1}^{1} x\Pi(dx)$ and adjusting the drift accordingly.

We can also prove that the process $X_t$ will have finite variation on any interval $[0, t]$. To do so, observe that as $X_t$ is a pure jump process, its total variation is given by the sum of the absolute value of its jumps, which can be written in terms of an integral involving the random measure, $N$. If $x_i$ are the jumps in the interval $[0, t]$, then

$$\sum |x_i| = \int_0^t \int_{\mathbb{R}/\{0\}} |x|N(dx, ds).$$

This integral converges if it meets the condition given in Theorem 2.3.3, namely $\int_0^t \int_{\mathbb{R}/\{0\}} (1 \wedge |x|)\Pi(dx)ds < \infty$, which is precisely the case we are discussing in this section. Thus $X_t$ will have finite variation.

### 2.4.3 Paths of Infinite Variation

We now consider the case where the Lévy measure satifies $\int_{\mathbb{R}/\{0\}}(1\wedge x^2)\Pi(dx) < \infty$, but $\int_{\mathbb{R}/\{0\}}(1 \wedge |x|)\Pi(dx) = \infty$. In this case, we can no longer define $X_t$ as in equation (2.6), because this integral would not converge. Instead, Lévy processes of this type are constructed in a different manner.

Define the set $B_\epsilon = \mathbb{R}/(-\epsilon, \epsilon)$ for $\epsilon > 0$. Define the measure $\Pi_\epsilon$ to be given by $\Pi_\epsilon(A) = \Pi(A \cap B_\epsilon)$. Observe that $\int_{\mathbb{R}/\{0\}}(1 \wedge |x|)\Pi_\epsilon(dx) < \infty$ for all $\epsilon$, and so we can define a Lévy process $X_t^\epsilon$ using the Poisson random measure $N_\epsilon$ induced by this measure. We will write this as

$$X_t^\epsilon = \int_0^t \int_{B_\epsilon} xN(dx, ds) - t\int_{B_\epsilon} x\Pi(dx). \tag{2.7}$$

The characteristic function of this process is

$$\mathbb{E}[e^{iuX_t^\epsilon}] = \exp\left(t\int_{B_\epsilon}(e^{iux} - 1 - iux)\Pi(dx)\right). \tag{2.8}$$

**Theorem 2.4.1.** *If $X_t^\epsilon$ is defined in equation (2.7), where the measure $\Pi$ satisfies $\int_{\mathbb{R}/\{0\}}(1 \wedge x^2)\Pi(dx) < \infty$, then $X_t^\epsilon$ is a square integrable martingale.*

This result can be found in [43].

To discuss the limit as $\epsilon \to \infty$, we need the following well known results, discussed at length in [51] and [52].

**Theorem 2.4.2.** *The space of real-valued, zero mean, right-continuous, square integrable martingales on $[0, T]$ is a Hilbert space with inner product given by $< X_t, Y_t >= \mathbb{E}[X_T Y_T]$.*

We continue by noting that under the norm given in Theorem 2.4.2, the sequence $X_t^\epsilon$ is Cauchy as $\epsilon \to 0$. The completeness of the space of square integrable martingales then gives us the existence of a process $X_t$ which satisfies $X_t^\epsilon \to X_t$ in $L^2$ as $\epsilon \to 0$. Using the Doob maximal inequality, we can get a deterministic subsequence of $\epsilon_i$ such that the convergence is uniform and pointwise almost surely, which is used to show that $X_t$ is still a Lévy process. [46] and [42] both provide excellent summaries of these results.

It is customary to write

$$X_t = \int_0^t \int_{\mathbb{R}/\{0\}} x \left( N(dx, ds) - \Pi(dx)ds \right),$$

where the right hand side is defined to be the square integrable martingale discussed above.

As convergence in $L^2$ implies weak convergence, we also see from equation (2.8) that the characteristic function of $X_t$ is given by

$$\mathbb{E}[e^{iuX_t}] = \exp\left( t \int_{\mathbb{R}/\{0\}} (e^{iux} - 1 - iux)\Pi(dx) \right).$$

Notice that this differs slightly from the characteristic function in the Levy-Khintchine theorem (Theorem 2.1.4). The difference can be explained by dividing the Lévy measure $\Pi$ into two separate measures, $\Pi = \Pi_1 + \Pi_2$ where $\Pi_1 = \Pi|_{\{|x| \geq 1\}}$ and $\Pi_2 = \Pi|_{\{|x|<1\}}$. Then one can create two independent Lévy processes, one with large jumps and finite variation and one with small jumps and infinite variation. This will cause the addition of the term $\mathbf{1}_{\{|x|<1\}}$ in the characteristic function. We should also mention at this point that the choice of $\{|x| \geq 1\}$ and $\{|x| < 1\}$ was com-

pletely arbitrary, any $\alpha < 0 < \beta$ could be used with a corresponding change in the characteristic function.

Finally, we comment on the total variation of the paths of $X_t$. Recall that the variation of $Y_t^\epsilon := \int_0^t \int_{B_\epsilon} xN(dx, ds)$ is finite if and only if $\int_{B_\epsilon}(1 \wedge |x|)\Pi(dx) < \infty$. As the jump structure of $X_t^\epsilon$ is the same as that of $Y_t^\epsilon$, the total variation of $X_t^\epsilon$ is at least as big as that of $Y_t^\epsilon$. As $\epsilon \to \infty$, $\int_{B_\epsilon}(1 \wedge |x|)\Pi(dx) \to \infty$, and so the total variation of $Y_t$ is going to $\infty$. Thus, the total variation of $X_t$ is going to $\infty$, and we can conclude that $X_t$ has infinite variation.

# Chapter 3

# The Hunt Variance Gamma Process

In this chapter we define a Hunt variance gamma process. This process is a time-homogeneous, space-inhomogeneous Markov process. We will first describe the variance gamma process, a Lévy process developed in the early 1990's. This process serves as a starting point for the development of the Hunt variance gamma process. Next we define the Hunt variance gamma process by describing its stochastic generator. We conclude this chapter by proving the existence and uniqueness of a Hunt variance gamma process.

## 3.1 The Variance Gamma Process

The variance gamma process provides several of the theoretical underpinnings of our later work, and so we will discuss it in some detail in this section. Much of this work was first described by Madan and Senata in [16] and later expanded and generalized in [17] and [18].

**Definition 3.1.1.** *A Lévy process $X_t$ is called a subordinator if it is an increasing process on $\mathbb{R}$.*

It should be clear from our discussion in Chapter 2 that the Lévy triplet of a subordinator will have several characteristics to insure that the process it describes is increasing. The Lévy triplet of a subordinator will satisfy $\mu \geq 0$, $\sigma = 0$, and

$\Pi(-\infty, 0) = 0$.

The idea of subordinating one random process by another was introduced by Bochner in [53] and later expanded in [54]. It is best described by the following theorem, with proof given in [42].

**Theorem 3.1.2.** *Let $Y_t$ be a Lévy process, and let $Z_t$ be a subordinator. Then the process*

$$X_t(\omega) := Y_{Z_t(\omega)}(\omega)$$

*is defined almost surely, and is a Lévy process.*

Using subordinated processes to model stock prices was first introduced in [55], and continued in [56], to name one instance. The variance gamma process is a continuation of these efforts.

We can now define a variance gamma process as a diffusion process subordinated by a gamma process. We let

$$Y_t = \theta t + \sigma W_t,$$

where $W_t$ is a standard brownian motion. This is a diffusion process with drift $\theta$ and volatility $\sigma$. Let $Z_t$ be a gamma process, with parameters $\mu$ and $\nu$. Recall that a gamma distribution with parameters $\mu$ and $\nu$ has density function given by

$$f(x) = \left(\frac{\mu}{\nu}\right)^{\frac{\mu^2}{\nu}} \frac{x^{\frac{\mu^2}{\nu}-1} \exp(-\frac{\mu}{\nu}x)}{\Gamma(\frac{\mu^2}{\nu})}, \text{ for } x > 0. \tag{3.1}$$

This density function has characteristic function

$$\int_{-\infty}^{\infty} e^{iux} f(x)dx = \left(\frac{1}{1 - iu\frac{\nu}{\mu}}\right)^{\frac{\mu^2}{\nu}},$$

which is infinitely divisible. Any infinitely divisible distribution can be used to create a Lévy process (see [26] for details), so we have a Lévy process $Z_t$ based on the gamma distribution. At time $t$, this process has a gamma distribution with parameters $\mu t$ and $\nu t$. We will denote this process by $Z_t^{(\mu,\nu)}$ below.

Using this notation, the variance gamma process $X_t$ with parameters $(\sigma, \nu, \theta)$ can then be written as

$$X_t = Y_{Z_t^{(\mu,\nu)}} = \theta Z_t^{(\mu,\nu)} + \sigma W_{Z_t^{(\mu,\nu)}}.$$

The distribution of $X_t$ has only three degrees of freedom, so we set the parameter $\mu$ to be equal to one by default. The result is a three parameter family, with parameters $(\sigma, \nu, \theta)$. Madan, Carr, and Chang showed several important features of this process in [18], which are summarized below.

First of all, one can find the density function of the variance gamma process by first conditioning on the value of the gamma process $Z_t^{(1,\nu)}$, and then integrating using the density function in equation (3.1). Upon doing this, we see that the probability density function of the variance gamma process is given by

$$f_{X_t}(x) = \int_0^\infty \frac{1}{\sigma\sqrt{2\pi u}} \exp\left(-\frac{(x-\theta u)^2}{2\sigma^2 u}\right) \frac{u^{\frac{t}{\nu}-1}\exp(-\frac{u}{\nu})}{\nu^{\frac{t}{\nu}}\Gamma(\frac{t}{\nu})} du.$$

We can use the same method to find the characteristic function, which is given by

$$\mathbb{E}[e^{iuX_t}] = \left(\frac{1}{1 - i\theta\nu u + (\sigma^2\nu/2)u^2}\right)^{t/\nu}. \tag{3.2}$$

The Lévy-Khintchine representation of the characteristic exponent can be found by writing the variance gamma process as the difference of two independent gamma

processes, as detailed in [18]. There we see that the variance gamma process is an infinite activity, finite total variation process with no diffusion component and having Lévy measure absolutely continuous to Lebesgue measure with Radon-Nikodym derivative

$$\Pi(x) = \frac{\exp(\theta x/\sigma^2)}{\nu|x|} \exp\left(-\frac{\sqrt{\frac{2}{\nu} + \frac{\theta^2}{\sigma^2}}}{\sigma}|x|\right). \tag{3.3}$$

There are several other parameterizations of the Lévy measure, we mention one other. Define

$$\begin{aligned}
\mu_p &= \frac{1}{2}\sqrt{\theta^2 + \frac{2\sigma^2}{\nu}} + \frac{\theta}{2} \\
\mu_n &= \frac{1}{2}\sqrt{\theta^2 + \frac{2\sigma^2}{\nu}} - \frac{\theta}{2} \\
\nu_p &= \left(\frac{1}{2}\sqrt{\theta^2 + \frac{2\sigma^2}{\nu}} + \frac{\theta}{2}\right)^2 \nu \\
\nu_n &= \left(\frac{1}{2}\sqrt{\theta^2 + \frac{2\sigma^2}{\nu}} - \frac{\theta}{2}\right)^2 \nu.
\end{aligned}$$

Then we can write the Lévy measure as

$$\Pi(x) = \begin{cases} \frac{\mu_n^2}{\nu_n} \frac{\exp(-\frac{\mu_n}{\nu_n}|x|)}{|x|} & \text{for } x < 0 \\ \\ \frac{\mu_p^2}{\nu_p} \frac{\exp(-\frac{\mu_p}{\nu_p}|x|)}{|x|} & \text{for } x > 0 \end{cases}.$$

This characterization is useful in understanding the relationship between the rate of positive jumps versus negative jumps.

One motivating factor in the development of the variance gamma process was the desire to be able to incorporate both skewness and kurtosis in asset returns. We can use the characteristic function in equation (3.2) to find the central moments of

the variance gamma process. These are given by

$$\begin{aligned}
\mathbb{E}[X_t] &= \theta t \\
\mathbb{E}[(X_t - \mathbb{E}[X_t])^2] &= (\theta^2\nu + \sigma^2)t \\
\mathbb{E}[(X_t - \mathbb{E}[X_t])^3] &= (2\theta^3\nu^2 + 3\sigma^2\theta\nu)t \\
\mathbb{E}[(X_t - \mathbb{E}[X_t])^4] &= (3\sigma^4\nu + 12\sigma^2\theta^2\nu^2 + 6\theta^4\nu^3)t + (3\sigma^4 + 6\sigma^2\theta^2\nu + 3\theta^4\nu^2)t^2.
\end{aligned}$$

We now attempt to give some intuitive explanation for the parameters of the variance gamma process. First, observe that the skewness of $X_t$ is given by

$$\frac{\mathbb{E}[(X_t - \mathbb{E}[X_t])^3]}{\mathbb{E}\left[(X_t - \mathbb{E}[X_t])^2\right]^{3/2}} = \theta\frac{2\theta^2\nu^2 + 3\sigma^2\nu}{(\theta^2\nu + \sigma^2)^{3/2}\sqrt{t}}.$$

$\sigma$ and $\nu$ are positive by definition, and so the sign of the skewness is completely determined by $\theta$. So $\theta > 0$ implies that the process will be right-skewed, while $\theta < 0$ implies left-skewness. If $\theta = 0$, the process has 0 skewness. In this case, the kurtosis is given by

$$\frac{\mathbb{E}[(X_t - \mathbb{E}[X_t])^4]}{\mathbb{E}[(X_t - \mathbb{E}[X_t])^2]^2} = 3(1 + \nu).$$

We can then interpret $\nu$ to represent excess kurtosis, see [57].

## 3.2 Definition of the Hunt Variance Gamma Process

We now wish to modify the variance gamma process into a new process that will no longer be Lévy. Recall that for a Lévy process $X_t$, we have that $X_t - X_s$ is independent of its history given by the sigma algebra $\mathscr{F}_s$. We wish to relax this assumption and instead create a process which is Markovian. To do this, we make

a slight change to the generator of the process. Before outlining the changes, we share some important results concerning generators of Lévy processes.

Recall that a strongly continuous semigroup is a family of bounded linear operators $P_t$ for $t \in [0, \infty)$ on a Banach space $\mathbf{X}$ which satisfy:

1. $P_t P_s = P_{t+s}$
2. $P_0 = I$ (the identity operator)
3. $\lim_{t \to 0} P_t f = f$ strongly .

For a Lévy process, we can define a continuous semigroup in the following manner. Let $\mathbf{X} = C_0$, where $C_0 = C_0(\mathbb{R})$ is the space of continuous functions $f : \mathbb{R} \to \mathbb{R}$ satisfying $\lim_{|x| \to \infty} f(x) = 0$. Equip this space with the sup-norm, where $||f|| = \sup_x |f(x)|$. This space is a Banach space (see [58]). For $f \in C_0$, and a Lévy process $X_t$, we can define the strongly continuous semigroup

$$P_t f(x) = \mathbb{E}[f(x + X_t)]. \tag{3.4}$$

The generator, or infinitesimal generator, of a strongly continuous semigroup is the linear operator $\mathscr{L}$ given by

$$\mathscr{L} f = \lim_{t \to 0} \frac{P_t f - f}{t}, \tag{3.5}$$

where once again the limit is taken in the strong sense from the metric. The generator is defined only on $f \in D(\mathscr{L})$, where $D(\mathscr{L})$ is the set where the limit on the right hand side of equation (3.5) converges.

The relationship between generators and strongly continuous semigroups is rich and has been studied extensively. For more information, we reference Hille ([59]) and Yosida ([60]).

A natural question in the discussion of generators is a description of $D(\mathscr{L})$. As this space is oftentimes difficult to identify, the identification of a core is important. A linear subspace $D_0$ of $\mathbf{X}$ is called a core of the operator $\mathscr{L}$ if $D_0 \subset D(\mathscr{L})$, and if the smallest closed extension of $\mathscr{L}|_{D_0}$ is equal to $\mathscr{L}$. For more on cores related to Lévy processes, see [61].

The following theorem can be found in [42], but was originally proven in [62] and [63]. It provides a description of the generator of a variance gamma process.

**Theorem 3.2.1.** *Let $X_t$ be a variance gamma process with Lévy measure $\Pi$. Then the semigroup described in equation (3.4) is a strongly continuous semigroup on $C_0$. The infinitesimal generator of this semigroup $\mathscr{L} : D(\mathscr{L}) \to C_0$ has $C_c^\infty$ as a core of $\mathscr{L}$ and $C_0^2 \subset D(\mathscr{L})$. Furthermore, for $f \in C_0^2$,*

$$\mathscr{L} f(x) = \int_{-\infty}^{\infty} (f(x+h) - f(x))\, \Pi(dh).$$

We are now in position to modify the generator of the variance gamma process. We wish to include some dependence on the value of the Lévy process, $X_t$. To do so, we form what is called in the literature a Lévy–type generator (see [64]). This is done by modifying the Lévy measure $\Pi$ to depend on the value of our process, so that for each $x$ we have a measure $\Pi(x, \cdot)$. Then we will define a linear operator $\mathscr{L} : D(\mathscr{L}) \to C_0$ by

$$\mathscr{L} f(x) = \int_{-\infty}^{\infty} (f(x+h) - f(x))\, \Pi(x, dh). \tag{3.6}$$

We consider the measure given by modifying the parameters of the variance gamma Lévy measure to depend on $x$, so that

$$\Pi(x, A) = \int_A \frac{\exp(\theta(x)y/\sigma(x)^2)}{\nu(x)|y|} \exp\left( -\frac{\sqrt{\frac{2}{\nu(x)} + \frac{\theta(x)^2}{\sigma(x)^2}}}{\sigma(x)} |y| \right) dy. \tag{3.7}$$

Note the similarities between this measure and the Lévy measure for a variance gamma process given in equation (3.3).

At this point we provide a fairly straightforward functional form of $\sigma$, $\mu$, and $\theta$. We choose three values, $x_1$, $x_2$, and $x_3$ with $x_1 < x_2 < x_3$, and then define

$$\sigma(x) = \begin{cases} \sigma_1 & \text{for } x \leq x_1 \\ \sigma_1 + (\sigma_2 - \sigma_1)\frac{x - x_1}{x_2 - x_1} & \text{for } x_1 < x \leq x_2 \\ \sigma_2 + (\sigma_3 - \sigma_2)\frac{x - x_2}{x_3 - x_2} & \text{for } x_2 < x \leq x_3 \\ \sigma_3 & \text{for } x_3 < x \end{cases}$$

so that $\sigma(x)$ is piecewise linear, continuous, and bounded. We define $\theta(x)$ and $\nu(x)$ in the same manner using three parameters for each function.

We will call the process resulting from this generator a Hunt variance gamma process (HVG process). A Hunt process is a strong Markov process which is quasi-left continuous (see [46]). In the next section we will show that the probability measure resulting from this generator has these characteristics, and so is a Hunt process.

## 3.3 Existence and Uniqueness

One question to be answered regarding this process is the question of existence. With the addition of spatial dependence in the generators measure, we lose the necessary Lévy property of independence. In this section, we show the existence of a process having generator given in equation (3.6).

To begin, we wish to more explicitly define the notion of existence. This can best be explained using what is known as the martingale problem. Before we explain the martingale problem, we will first address some preliminaries.

We introduce the notation $D$ to represent the space of all cádlàg functions in $\mathbb{R}^+$, i.e.

$$D = \{\omega : [0,\infty) \to \mathbb{R} : \omega \text{ is right continuous and } \lim_{s\uparrow t} \omega(s) \text{ exists}\}.$$

We give $D$ a metric topology, known as the Skorohod topology, by defining a metric in the following way:

Let $\Lambda$ be the set of all bijective, monotonicly increasing Lipschitz functions $\lambda : [0,\infty) \to [0,\infty)$ with the property that

$$||\lambda||_\Lambda = \sup_{s,t\geq 0} \left|\log \frac{\lambda(s)-\lambda(t)}{s-t}\right| < \infty.$$

Then for any $\omega_1, \omega_2 \in D$, $\lambda \in \Lambda$, and $u \geq 0$ we define

$$\tilde{d}(\omega_1,\omega_2,\lambda,u) = \sup_{t\geq 0} |\omega_1(t\wedge u) - \omega_2(\lambda(t)\wedge u)| \wedge 1.$$

Finally, we can define the Skorohod metric $d$ on $D$ given by

$$d(\omega_1,\omega_2) = \inf_{\lambda\in\Lambda}\left(||\lambda||_\Lambda \vee \int_0^\infty e^{-u}\tilde{d}(\omega_1,\omega_2,\lambda,u)du\right).$$

The Skorohod metric and topology is a generalization of the sup-norm topology on the set of continuous functions, $C_{[0,\infty)}$. This metric is unsuitable for cádlág functions, because convergence in the sup-norm would require jumps to occur at the exact same time for convergence, as illustrated in the example below.

**Example 3.3.1.** *Let $\omega_n : [0,\infty) \to \mathbb{R}$ be given by*

$$\omega_n(x) = \begin{cases} 0 & \text{for } x < 1 - \frac{1}{n} \\ \\ 1 & \text{for } x \geq 1 - \frac{1}{n} \end{cases}.$$

*Let $\omega(x) = \mathbf{1}_{\{x \geq 1\}}$. Under the max-norm, $||\omega - \omega_n|| = \sup_x |\omega(x) - \omega_n(x)| = 1$, and so $\omega_n$ does not converge to $\omega$.*

*To show that $\omega_n \to \omega$ in the Skorohod topology, we distort the time scale using the function $\lambda_n(t) = \frac{1}{1-1/n}t$. Observe that for this function, $\omega(\lambda_n(t)) = \omega_n(t)$ for all $t$. Furthermore, if $u < 1 - 1/n$ or $u \geq 1$, then*

$$\sup_{t \geq 0} |\omega(\lambda_n(t) \wedge u) - \omega_n(t \wedge u)| = 0$$

*and so*

$$\int_0^\infty e^{-u} \tilde{d}(\omega_n, \omega, \lambda_n, u) du \leq \int_{1-1/n}^1 e^{-u} du \leq \frac{1}{n}.$$

*We can also see that*

$$||\lambda_n||_\Lambda = \log\left(\frac{1}{1-1/n}\right),$$

*and so*

$$\lim_{n\to\infty} d(\omega_n, \omega) \leq \lim_{n\to\infty} \left(\log\left(\frac{1}{1-1/n}\right) \vee \frac{1}{n}\right) = 0$$

*under the Skorohod metric.*

More information about convergence under the Skorohod metric can be found in [65], along with several other sources.

The space $D$ of cádlág functions is a complete separable metric space using this metric (see [66]). We will be considering stochastic processes in $D$, and using the usual notation where for $t \in [0, \infty)$, $X_t : D \to \mathbb{R}$ is given by $X_t(\omega) = \omega(t)$. We can define the $\sigma$ algebra

$$\mathscr{F} = \sigma(X_s : s \in [0, \infty))$$

and the filtrations

$$(\mathscr{F}_t) = \sigma(X_s : s \leq t).$$

Using this notation, we explain the martingale problem. Let $M(D)$ denote the space of probability measures on $D$, and let $B(\mathbb{R})$ denote the space of measurable and bounded functions on $\mathbb{R}$. Let $\mathscr{L} : D(\mathscr{L}) \to B(\mathbb{R})$ where $D(\mathscr{L}) \subset B(\mathbb{R})$ is the domain of $\mathscr{L}$. Finally, let $\mu$ be a probability measure on $\mathbb{R}$. A probability measure $\mathbb{P} \in M(D)$ is called a solution to the martingale problem starting with distribution $\mu$ for the operator $\mathscr{L}$ if:

1. $\mathbb{P}(X_0 \in A) = \mu(A))$

2. for every $f \in D(\mathscr{L})$,

$$f(X_t) - \int_0^t \mathscr{L} f(X_s) dx$$

is a martingale with respect to $(\mathscr{F}_t)$.

A martingale problem is called well–posed if for every starting distribution $\mu$ there exists a unique solution to the martingale problem.

The martingale problem was first introduced by Stroock and Varadhan (see [67]) for generators associated with diffusion processes, and later expanded to include theory of Lévy processes in [68]. The following result can be found in [64].

**Theorem 3.3.2.** *If the martingale problem is well–posed, then the probability space* $(D, \mathscr{F}, \mathbb{P}, \{X_t\})$ *is a strong Markov process.*

To show that the Hunt variance gamma process is well posed, we follow the approach given in [69]. Bass shows the following:

**Theorem 3.3.3.** *Suppose that*

1. $$\sup_x \int (1 \wedge y^2)\Pi(x, dy) < \infty, \text{ and} \tag{3.8}$$

2. *for each* $f \in C_0^2$, $\mathscr{L}f(x)$ *is uniformly continuous in* $x$.

*Then for every* $x_0$ *there exists a solution to the martingale problem for* $L$ *starting with distribution* $\delta_{x_0}$.

It is straightforward to show that part (1) of this theorem is applicable to the Hunt variance gamma process. We know from the Lévy-Khintchine theorem (Theorem 2.1.4) that for any single $x$, $\int (1 \wedge y^2)\Pi(x, dy) < \infty$. For fixed $x$ this integral reduces to the characteristic exponent of a variance gamma process, and so this integral can be evaluated and is given by the log of equation (3.2), which is a continuous function in $\theta$, $\nu$, and $\sigma$. In the case of the VG Hunt process, $\theta$, $\nu$, and $\sigma$ are continuous and bounded functions of $x$, and so the integral in equation (3.8) is constant except on a compact set, where it is continuous. Thus it is bounded.

To show that part (2) of this theorem applies to the Hunt VG process, we will define, for any $f \in C_0^2$, the operator $\mathscr{A}_f(x, y)$ given by

$$\mathscr{A}_f(x, y) = \int_{\mathbb{R}/\{0\}} (f(x + h) - f(x)) \, \Pi(y, dh).$$

It will also be useful to define the function $\chi(y)$, given by

$$\chi(y) = x_1 \mathbf{1}_{x \leq x_1}(y) + y \mathbf{1}_{x_1 \leq x \leq x_3}(y) + x_3 \mathbf{1}_{x_3 \leq x}(y).$$

Observe that because of our definition of the functions $\sigma$, $\nu$, and $\theta$ in Section 3.2, the relationship

$$\mathscr{L} f(x) = \mathscr{A}_f(x, \chi(x))$$

will hold.

We will first show the following two lemmas, and then use them to show that part (2) of Theorem 3.3.3 is satisfied for the Hunt VG process. In all cases, assume $f$ is a fixed element of $C_0^2$, and let $\mathscr{A} = \mathscr{A}_f$.

**Lemma 3.3.4.** *The mapping $x \to \mathscr{A}(x, \chi(y))$ is uniformly continuous, independent of $y$.*

*Proof.* Let $\epsilon > 0$ be given. We need to show that

$$\sup_{y \in I} |\mathscr{A}(x_1, y) - \mathscr{A}(x_2, y)| < \epsilon \tag{3.9}$$

if $x_1$ and $x_2$ are close. Here $I$ is the range of $\chi$.

To show this, write out the above statement in terms of the definition of $\mathscr{A}$. We see that the statement on the left of equation (3.9) is

$$\int_{\mathbb{R}/\{0\}} (f(x_1 + h) - f(x_1)) - (f(x_2 + h) - f(x_2)) \, \Pi(\chi(y), dh),$$

which we split into two integrals. Let

$$I_1 = \int_{B(0,r)/\{0\}} (f(x_1+h) - f(x_1)) - (f(x_2+h) - f(x_2))\Pi(\chi(y), dh),$$

and let

$$I_2 = \int_{\mathbb{R}/B(0,r)} (f(x_1+h) - f(x_1)) - (f(x_2+h) - f(x_2))\,\Pi(\chi(y), dh).$$

Then by Taylor's theorem and $f \in C_0^2$,

$$I_1 \leq C \int_{B(0,r)/\{0\}} h\Pi(\chi(y), dh).$$

From our definition of $\Pi$ in equation (3.7), we can see that $h\Pi(\chi(y), dh)$ is a bounded function, and that his bound can be chosen independent of $y$. Thus by choosing $r$ small enough, we can bound $I_1$.

Bounding $I_2$ is similarly straightforward. For $h \in [r, R]$, the function $f$ is uniformly continuous and $\Pi$ is bounded (independent of $y$), and so if $|x_1 - x_2| < \delta$ that piece of the integral can be made arbitrarily small. Finally, $f\Pi$ is integrable, and so the integral outside of $R$ can be made arbitrarily small by choosing $R$ large.

□

**Lemma 3.3.5.** *The operator $T : \mathbb{R} \to C_0(\mathbb{R})$ given by $y \to \mathscr{A}(x, \chi(y))$ is uniformly continuous.*

*Proof.* Consider that

$$\begin{aligned}
&\mathscr{A}(x,\chi(y_1)) - \mathscr{A}(x,\chi(y_2)) \\
&= \int_{\mathbb{R}/\{0\}} (f(x+h)-f(x)) \left(\Pi(\chi(y_1),dh) - \Pi(\chi(y_2),dh)\right) \\
&= \int_{B(0,r)/\{0\}} (f(x+h)-f(x)) \left(\Pi(\chi(y_1),dh) - \Pi(\chi(y_2),dh)\right) \\
&\qquad + \int_{B(0,R)/B(0,r)} (f(x+h)-f(x)) \left(\Pi(\chi(y_1),dh) - \Pi(\chi(y_2),dh)\right) \\
&\qquad + \int_{\mathbb{R}/B(0,R)} (f(x+h)-f(x)) \left(\Pi(\chi(y_1),dh) - \Pi(\chi(y_2),dh)\right) \\
&= I_1 + I_2 + I_3,
\end{aligned}$$

where $I_1$, $I_2$, and $I_3$ are the three integrals shown.

$I_1$ and $I_3$ can be made arbitrarily small by choosing $r$ small and $R$ large, as was done in the previous lemma. $I_2$ is also easily bounded by

$$|I_2| \;\leq\; C \int_{B(0,R)/B(0,r)} \left(\Pi(\chi(y_1),dh) - \Pi(\chi(y_2),dh)\right).$$

As $\Pi$ is a continuous function and is being integrated on a compact set, it can be made arbitrarily small by choosing $y_1$ and $y_2$ near each other.

Finally, none of the arguments made above rely on the specific value of $x$ chosen. Thus if we take the supremum over $x$ of $|\mathscr{A}(x,\chi(y_1)) - \mathscr{A}(x,\chi(y_2))|$, we can make it arbitrarily small if $|y_1 - y_2|$ is small. □

With these lemmas, it is straightforward to prove that the Hunt variance gamma process satisfies part (2) of Theorem 3.3.3. To show that $\mathscr{L}f$ is uniformly

continuous, we observe that

$$\begin{aligned} |\mathscr{L}f(x_1) - \mathscr{L}f(x_2)| &= |\mathscr{A}(x_1, \chi(x_1)) - \mathscr{A}(x_2, \chi(x_2))| \\ &\leq |\mathscr{A}(x_1, \chi(x_1)) - \mathscr{A}(x_2, \chi(x_1))| \\ &\quad + |\mathscr{A}(x_2, \chi(x_1)) - \mathscr{A}(x_2, \chi(x_2))|. \end{aligned}$$

Lemma 3.3.4 says that if $|x_1 - x_2|$ is small, the first expression is small. Lemma 3.3.5 says the same about the second.

Once existence of a solution to the martingale problem has been established, it is a simple matter to get uniqueness for the martingale problem we have described. In [66], it is shown that if a solution to the martingale problem exists for each initial distribution $\delta_x$, a solution exists for any distribution $\mu$. A uniqueness result applying to our problem can be found in [68]. It says:

**Theorem 3.3.6.** *Assume that $\mathscr{L}f(x)$ is defined as in equation (3.6). Furthermore, assume that*

$$\int_A \left(e^{iuh} - 1 - iuh\mathbf{1}_{\{|h|<1\}}\right) \Pi(x, dh)$$

*is bounded and continuous for all Borel sets $A \subset \mathbb{R}$. Then the solution $\mathbb{P}$ to the martingale problem is unique.*

This theorem, combined with Theorem 3.3.2 shows that the solution $(X_t, \mathbb{P}_t)$ is a strong Markov process. It is also shown in [69] that the solution is a Feller process.

At this point, we should note that it would be straightforward to construct several other Hunt processes in this manner. Here we allowed the parameters of

a variance gamma process to depend continuously on $x$ in a linear manner. Note however, that the only properties we used to prove existence and uniqueness was that the parameters depended continuously on $x$, and that they were only allowed to take on values in a compact set. So long as these two properties are preserved, we could generate many other Hunt processes based on the variance gamma process. One way to do this is to let $\theta$, $\nu$, and $\sigma$ be more complicated functions of $x$, instead of piecewise linear.

We also note that this approach could be used on other types of Lévy processes. The characteristics of the measure $\Pi$ are general to all Lévy measures, and so the same techniques could be employed. Slight modifications would be needed if the process had infinite variation instead of finite variation (for example, the generator would have a derivative term in it), but these present no real obstacles.

# Chapter 4

## Computation Using the Hunt Variance Gamma Process

In this chapter we will describe a method to compute probabilities from a Hunt variance gamma process. This is done by constructing a Markov chain which approximates the behavior of the Hunt variance gamma process. We will describe how to construct this chain, investigate the convergence rate of this approximation scheme, and finally use the Markov chain to find option prices. We also calibrate a Hunt variance gamma process to fit the S&P 500 option surface on a variety of days, and investigate the resulting goodness of fit.

## 4.1 Markov Chain Approximations

We now will explain how to price options using the Hunt variance gamma process described earlier. We begin with a risk-neutral stock model, where the stock price $S_t$ at time $t$ is given by

$$S_t = S_0 e^{rt + X_t - \int_0^t \omega(X_s) ds}. \tag{4.1}$$

Here $S_0$ is the current stock price, $r$ is the risk free interest rate, and $X_t$ is a hunt variance gamma process. The integral of $\omega(X_s)$ exists so that the discounted process is a martingale in the approximation process described below. We define

$$\omega(x) = \frac{-1}{\nu(x)} \log\left(1 - \theta(x)\nu(x) - \frac{1}{2}\sigma(x)^2\nu(x)\right),$$

and note that if $X_t$ is a variance gamma process with Lévy measure $\Pi(x, dy)$ (for fixed x) then $e^{X_t - \omega(x)t}$ is a martinagale. This can be seen using the Lévy process properties of independence and stationary increments. Expectations can be computed using the characteristic function of a variance gamma process shown in equation (3.2).

Note that in this model, we have directly modeled the risk-neutral price process instead of first modeling the physical measure and then converting to a risk neutral process. Under the risk-neutral measure, the discounted price process is a martingale. There is a well established link between martingales and arbitrage-free pricing rules, namely that any martingale measure equivalent to the true probability measure specifies a pricing rule which is arbitrage free. This fact was first established for discrete time models in [70], and was later proved for continuous time models in [71] and [72]. Since this introduction, a large amount of work has been done. More detailed summaries can be found in [73], [74], and [75].

Under a risk-neutral measure, European option prices can be found by computing expectations of their payoffs at expiration. If a European option has terminal payoff $H(S_T)$, the time 0 cost of this option is given by

$$e^{-rT}\mathbb{E}[H(S_T)].$$

For call options, $H(x) = (x - K)^+$, where $x^+ = \max\{x, 0\}$. Put options have payout given by $H(x) = (K - x)^+$. In both of these contracts, $K$ is an agreed upon constant, called the strike price.

Usually we can compute these expectations using the characteristic function

of the driving random process, $\mathbb{E}[e^{iuX_t}]$. To do so we use Fourier transform methods detailed in [15]. This is convenient for both Lévy and Sato processes for example, because their characteristic function is known analytically (see Theorem 2.1.4 and equation (1.2)). However, we have no information about the characteristic function of the Hunt variance gamma process because of the spatial inhomogeneity of $X_t$, so this method will not work.

Instead, we use a new approach developed by Mijatović and Pistorius in 2011 (see [76]). In this paper, the authors describe a method to construct a finite–state continuous time Markov chain approximation for processes with known generators. We will construct the Markov chain approximation for the Hunt variance gamma process, and then compute expectations and option prices using the approximation.

There are two major steps in the approximation process. First, one needs to specify the (finite) state space upon which the process will be approximated. This space will be denoted $G = \{s_1, \ldots, s_n\}$. After specifying a state space, we will define the generator matrix for a Markov chain on that state space, which will be denoted by $\Lambda$. This generator matrix completely defines the Markov process.

The most obvious choice for $G$ is to use a uniform grid over some bounded set. This is computationally inefficient, so a non-uniform approach is adapted. There are two goals in choosing a non-uniform grid. First, we wish to minimize error due to the truncation of an unbounded state space into a necessarily bounded state space. This implies that $s_n - s_1$ should be as large as possible. However, there is high probability that the stock remains near its starting location, and so a finer resolution is desired in this location. Note that the idea of an adaptive mesh in option pricing

has been studied in the past. Early work includes [77]. In what follows, we use the same approach as Mijatović and Pistorius in [76], who based their method on an algorithm from [78].

The algorithm is as follows. Choose a lower bound $a$ and an upper bound $b$ for the state space. Use the current stock price, $S_0$, and let $n$ be the total number of states desires. Finally, choose a density parameter $g$. Then set

$$\begin{aligned} c_1 &= \text{arcsinh}\left(\frac{a - S_0}{g}\right) \\ c_2 &= \text{arcsinh}\left(\frac{b - S_0}{g}\right) \end{aligned}$$

Let the lower part of the grid, $\{s_1, \ldots, s_{n/2}\}$, be given by

$$s_k = S_0 + g\text{sinh}\left(c_1(1 - (k-1)/(n/2-1))\right).$$

for $k \in \{1 \ldots, n/2\}$. We let the upper part of the grid be given by

$$s_{n/2+k} = S_0 + g\text{sinh}\left(c_2 2k/M\right).$$

The density parameter controls the concentration of points around the middle point, $S_0$. High values of $g$ result in more uniform spacing, while lower values lead to a higher concentration of points around $S_0$. A sample grid is given in Figure 4.1.

With the state space $G = \{s_1, \ldots, s_n\}$ constructed, we now turn our attention to the generator matrix $\Lambda$ of the Markov chain. This is carried out in two steps. First, we will construct the generator, $\Lambda_J$ of the jump component of the discretization of the stochastic process, and then we will construct $\Lambda_C$, the continuous part.

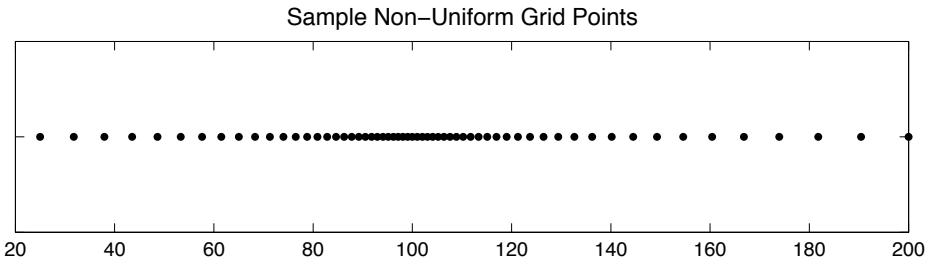


Figure 4.1: This is a sample non-uniform grid generated by the algorithm described in Section 4.1. Here we used as parameters $S_0 = 100$, $n = 60$, $a = 25$, $b = 200$, and $g = 10$.

To construct $\Lambda_J$, we start by looking at the jump sizes required to jump from $s_i$ to $s_k$. For each $s \in G$, we define the set

$$G_s = \{\log(s_j/s)\} \text{ for } j = \{1, \ldots, n\}.$$

This set gives the change needed in $X_t$ to jump from $s$ to any other point in $G$. Consider now the set $G_{s_i}$ and label it $G_{s_i} = \{j_1, \ldots, j_n\}$, with $j_1 < j_2 < \ldots < j_n$.

To compute the $(i, k)$ entry of $\Lambda_J$ $(i \neq k)$ we integrate the jump measure on a set surrounding the appropriate jump size. The $(i, k)$ entry of $\Lambda_J$ represents the jump intensity of a jump from $s_i$ to $s_k$, and so we set

$$\Lambda_J(i, k) = \int_{\alpha(j_k)}^{\alpha(j_{k+1})} \Pi(\log(s_i), dy)$$

for $i \neq k$.

Here $\alpha : G \to \mathbb{R}$ with $j_{k-1} < \alpha(j_k) < j_k$ for all $k$. Any function satisfying this requirement can be used. The convenient choice is to simply let

$$\alpha(j_k) = \frac{j_{k-1} + j_k}{2}.$$

We also set $\alpha(j_1) = -\infty$ and $\alpha(j_{n+1}) = \infty$. This function partitions the jump space $\mathbb{R}$ and we then integrate the jump measure to approximate the jump intensity.

Finally, we set

$$\Lambda_J(i,i) = -\sum_{k \neq i} \Lambda_J(i,k).$$

Markov generator matrices have the property that each row sums to one, so this condition assures that $\Lambda_J$ will be a generator matrix. Also, for $i \in \{1, n\}$, we set $\Lambda(i,k) = 0$ for all $k$. This will cause the left and right endpoint of $G$ to be absorbing states in the Markov chain approximation.

Next, we construct the continuous part of the generator matrix, $\Lambda_C$. This portion assures us that the first and second instantaneous moments of the Markov chain approximation match the moments of $S_t$. If $X_t$ is the Markov chain approximation process starting at $S_0$ which we are currently constructing, we require

$$\mathbb{E}[(S_t - S_0)^j] = \mathbb{E}[(X_t - S_0)^j] + o(t).$$

This Markov chain approximation must hold as $S_t$ changes values, and so we require the above equality to hold for all $S_0 \in G$, not just the initial stock price.

In order for this condition to hold, $\Lambda_C$ must be chosen so that the process generated by $\Lambda_J + \Lambda_C$ has this property. This means that the following two conditions must hold

$$\begin{aligned}
\sum_{k=1}^{n} \Lambda_C(i,k)(s_k - s_i) &= rs_i - \sum_{k=1}^{n} \Lambda_J(i,k)(s_k - s_i) \\
\sum_{k=1}^{n} \Lambda_C(i,k)(s_k - s_i)^2 &= s_i^2 C(s_i) - \sum_{k=1}^{n} \Lambda_J(i,k)(s_k - s_i)^2
\end{aligned}$$

Here $C(s_i)$ is chosen to be the instantaneous rate of change of the expected

value of $(S_t - S_0)^2$) for an exponential variance gamma process with Lévy measure $\Pi(\log(s_i), dy)$. This can be calculated using the characteristic equation of a variance gamma process shown in equation (3.2), and is given by

$$C(s) = s^2 \left( \frac{2}{\nu} \log(1 - \theta\nu - \sigma^2\nu/2) - \frac{1}{\nu}(1 - 2\theta\nu - 2\sigma^2\nu) \right).$$

Here $\nu$ is actually $\nu(\log(s))$, and $\theta$ and $\sigma$ are given in a similar manner.

$\Lambda_C$ must also be chosen in such a way that $\Lambda_C + \Lambda_J$ is a generator, which means that

$$\sum_{k=1}^{n} \Lambda_C(i,k) = 0$$

and

$$\Lambda_J(i,k) + \Lambda_C(i,k) \geq 0$$

for all $i$ and $k$.

The generator $\Lambda$ of the Markov chain approximation is then given by setting $\Lambda = \Lambda_J + \Lambda_C$. A Markov chain matrix can be obtained from the generator using matrix exponentiation. Many numerical software programs have packages designed for matrix exponentiation. Matlab uses the Padé approximation with scaling and squaring, see [79] for a description.

Pricing options using the generator is now a straightforward process. Let $\mathbf{s} = [s_1, s_2, \ldots, s_n]^T$, a column vector of the state space. Let $\mathbf{1}_k$ be a zero row vector with a one in the $k$-th entry. If the current stock price $S_0 = s_k$, then the price of a European call option $C(K,T)$ with strike $K$, expiration time $T$, and interest rate $r$ is given by the expression

$$C(K,T) = e^{-rT} \mathbf{1}_k e^{T\Lambda} (\mathbf{s} - \mathbf{K})^+.$$

A put option has price $P(K,T)$ given by

$$P(K,T) = e^{-rT}\mathbf{1}_k e^{T\Lambda}(\mathbf{K}-\mathbf{s})^+.$$

Here $\mathbf{K}$ is a vector of $K$'s having the same size as $\mathbf{s}$, and the $^+$ operation is applied to each component individually.

## 4.2 Convergence and Error Estimates

We wish to show that the Markov chain approximation outlined in the previous section converges to the process given in equation (4.1). In this context, we are discussing weak convergence of measures on the space of cádlág function under the Skorohod topology. Note that if $X_t^{(n)} \to S_t$ weakly, then

$$\mathbb{E}[H(X_T^{(n)})] \to \mathbb{E}[H(S_T)]$$

for bounded and continuous functions $H$, and so we can accurately evaluate European option prices in the limit.

To show weak convergence, we once again follow the approach done in [76]. We define $\Lambda^{(n)}$ as above, where $n$ shows the number of discrete states (so that $|G| = n$). We let $G^{(n)}$ be the grid generated, where $G^{(n)} = \{s_1^{(n)}, \ldots, s_n^{(n)}\}$. We also assume that as $n \to \infty$, $s_1^{(n)} \to 0$ and $s_n^{(n)} \to \infty$. Using this notation, we define for f in a core of $\mathscr{L}$,

$$\epsilon_n(f) = \max_{s\in G} \left|\Lambda^{(n)} f_n(s) - \mathscr{L}f(s)\right|.$$

Here $f_n = f|_{G^{(n)}}$.

A theorem of Ethier and Kurtz ([66]) says that if

$$\epsilon_n(f) \to 0 \tag{4.2}$$

then the sequence $X_t^{(n)}$ will converge weakly to $S_t$, and so a study of $\epsilon_n(f)$ will give the desired result.

Before we do this, notice that if $\epsilon_n(f) \to 0$ for all $f$, it must be the case that $G^{(n)}$ covers $\mathbb{R}^+$. If, for example, there exists an open set $(a,b) \subset \mathbb{R}^+$ where $G^{(n)} \cap (a,b) = \emptyset$ for large $n$, then the condition that $\epsilon_n(f) \to 0$ can not hold. To see this, observe that there exists a continuous, infinitely differentiable, nonnegative function $f$ having support in $(a,b)$. For this $f$, $\Lambda^{(n)} f_n(x) \equiv 0$, because $f = 0$ on $G^{(n)}$. However, $\mathscr{L} f(x) \neq 0$. This shows what it means for $G^{(n)}$ to cover $\mathbb{R}^+$. Observe also that this same argument can be applied to show that as $n \to \infty$, $s_1^{(n)} \to 0$ and $s_n^{(n)} \to \infty$.

To show that $\epsilon_n(f) \to 0$, we need to know the generator of the process $S_t$ given in equation (4.1). This will differ from the generator given in equation (3.6) because of the exponential and drift terms. It will also be convenient to denote the measure of the variance gamma Hunt process in terms of the stock value $S_t$ instead of in terms of $X_t$, so that for fixed $S_0$, $\Pi(s, dy)$ is actually referring to $\Pi(\log(\frac{s}{S_0}), dy)$ under the previous notation. A similar modification is done to $\omega$. Using this notation, the generator $\mathscr{L}$ for $S_t$ is given by

$$\mathscr{L} f(s) = (r - \omega(s))\, s \frac{\partial f}{\partial s} + \int_{\mathbb{R}/\{0\}} (f(se^y) - f(s))\, \Pi(s, dy).$$

Furthermore, we look at the class of functions $f : [0, \infty) \to \mathbb{R}$ which vanish at both 0 and infinity. Details on this can be found in [80].

To show that $\epsilon_n(f)$ goes to 0, we begin by ignoring the diffusion term of $\mathscr{L}$ which will be taken care of by the conditions placed on $\Lambda_C$. Instead, we look only at the jump measure and $\Lambda_J$.

We can write

$$\Lambda_J^{(n)} f_n(s_i) = \sum_{k \neq i} (f(s_k) - f(s_i)) \int_{\alpha(j_k)}^{\alpha(j_{k+1})} \Pi(s_i, dy),$$

and so

$$\begin{aligned} \Lambda_J^{(n)} f_n(s_i) - \mathscr{L} f(s_i) &= \sum_{k \neq i} \int_{\alpha(j_k)}^{\alpha(j_{k+1})} (f(s_k) - f(s_i e^y)) \, \Pi(s_i, dy) \\ &\quad - \int_{\alpha(j_i)}^{\alpha(j_{i+1})} (f(s_i e^y) - f(s_i)) \, \Pi(s_i, dy). \end{aligned}$$

The first integral in the above equation goes to 0 as $n \to \infty$ because of several factors. First, $f$ vanishes at both 0 and infinity and is bounded. The same is true for $f'$. We then use Taylor's theorem and properties of $G^{(n)}$ as it is described above to show that the integral goes to 0 as $n \to \infty$ independent of $s_i \in G^{(n)}$. This procedure is done in detail in [81] for a similar process. It is easy to see that the second integral goes to 0 as $n \to \infty$, because $\alpha(j_i)$ and $\alpha(j_{i+1})$ both go to 0 and $f(s_i e^y) - f(s_i)$ has a finite integral.

In this manner, we show that $\epsilon_n(f) \to 0$ as $n \to \infty$. As stated above, this tells us that $X^{(n)_t}$ converges to $S_t$ weakly, and so we can take limits to price European options which are bounded as functions of $S_T$. The boundedness condition theoretically excludes call options (which are unbounded), but in practice we truncate the payoff without losing any noticeable accuracy.

Recall also that the weak convergence is weak convergence of a measure on the

space of cádlág functions, and so the expectation of any continuous functional from this space will converge. This means that we can price options which are functions not only of the stock price at time $T$, but also functionals which are path dependent, so long as they are continuous maps under the Skorohod topology. Mijatović and Pistorius show in [76] that barrier options satisfy this continuity requirement. More work needs to be done to show that other derivatives, such as Asian options, binary options, and other exotic options (see [82]), satisfy this requirement.

We will now discuss the rate of convergence. Recall that $G^{(n)} = \{s_1^{(n)}, \ldots, s_n^{(n)}\}$, and that to jump from $s_i^{(n)}$ to $s_k^{(n)}$, $S_t$ must change by $j_k$. For a given $n$, let

$$h(n) = \max_i |s_{i+1} - s_i|,$$

the mesh size in the discretization.

Also, for a given $s_i^{(n)}$ define

$$L\left(s_i^{(n)}\right) = j_1$$

which is the smallest possible jump and

$$U\left(s_i^{(n)}\right) = h_n,$$

the largest possible jump.

Using this notation, we define

$$k(n) = \max_{s_i^{(n)} \in G^{(n)}} \int_{\mathbb{R}/[L(s_i^{(n)}), U(s_i^{(n)})]} \Pi(s_i^{(n)}, dh),$$

which corresponds to the total jump measure which is not included in the construction of $\Lambda^{(n)}$.

Using this notation we get the following theorem.

**Theorem 4.2.1.** *Suppose that $f$ is Lipshitz continuous with compact support. Suppose furthermore that the sequence of grids, $G^{(n)}$, satisfies*

$$\lim_{n\to\infty} h(n) = \lim_{n\to\infty} k(n) = 0.$$

*Then for large $n$ and for all $s_i^{(n)} \in G^{(n)}$, there exists constants $c_1$ and $c_2$ such that*

$$\left|\mathbb{E}\left[e^{-rT} f(S_T)\right] - \mathbb{E}\left[e^{-rT} f(X_T^{(n)})\right]\right| \leq c_1 h(n) + c_2 k(n).$$

This theorem with its corresponding proof can be found in [76]. Note that this theorem is a special case of that one, because

$$\max_x \int_{\mathbb{R}/\{0\}} |y| \Pi(x, dy) < \infty.$$

Figure 4.2 shows the rate of convergence for option prices under a variance gamma process. The variance gamma process can be simulated exactly (see [83]), and so exact option prices were computing using a Monte Carlo simulation. The upper and lower bounds were fixed, so that $k(n)$ is constant. The figure shows that the log error decays linearly with $\log(h(n))$ with an approximate slope of 1. Here $G^{(n)}$ is calculated using the method detailed earlier in this chapter.

## 4.3 Calibration

We can use the approach described in Section 4.1 to price European options. We know that the option prices generated from a given set of parameters will be arbitrage free because the discounted price process is a martingale ([84]). However, every set of parameters for the Hunt variance gamma process will generate an

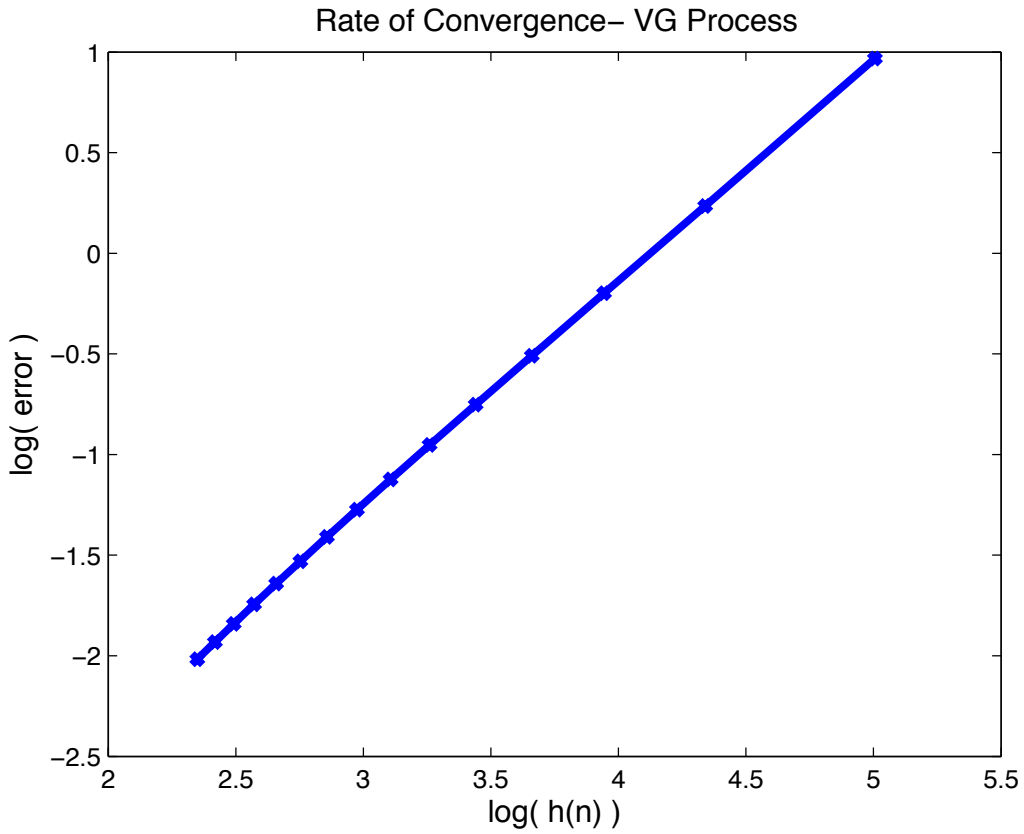


Figure 4.2: This figure plots the log error of the price of a European call option with the log of the maximum mesh size. The mesh was generated using the algorithm in this chapter for $G^{(n)}$. The stock value is given by $S_t = S_0 \exp((r+\omega)t + X_t)$ where $X_t$ is a variance gamma process and $\omega$ forces the process to be a martingale. The variance gamma process has parameters $\sigma = 0.25$, $\nu = 0.1$, and $\theta = 0.35$. Other necessary parameters are $r = 0.01$, $T = 1$, $S_0 = 1000$, and $K = 1000$.

equivalent martingale measure, and so any set of parameters will generate option prices which are free of static arbitrage. We cannot hedge option payouts because markets are incomplete, and so a no-arbitrage assumption alone is insufficient to chose parameters. This is true for any jump process, and so we use a calibration procedure to choose parameters for these types of models.

Calibration consists of choosing parameters for a model which give prices consistent with the option prices which are currently being traded in the market. In other words, the model parameters are chosen to fit the observable market data. In this way we hope to incorporate as much market information as possible into the model.

To calibrate a model described by the parameters $\Theta$, we will attempt to minimize the least-square difference between model prices and market prices. We assume there are $N$ options trading in the market, and that option $i$ has price $O_i$. For given values of $\Theta$, we assume that the model gives option prices $O_i^{\Theta}$. We then choose $\Theta$ by letting

$$\Theta^* = \arg\min_{\Theta} \sum_{i=1}^{N} \left(O_i - O_i^{\Theta}\right)^2. \tag{4.3}$$

This is a common approach to calibrating a model (see [85] or [86] for examples). The error function to be minimized can be adjusted to include weights based on liquidity indicators such as the bid-ask spread. Other criteria for calibration is discussed in [87].

In what will follow, we minimize equation (4.3) when model prices come from a variance gamma and a Hunt variance gamma process. We do this using a built

in MATLAB function minimizing routine. In this case, we used the **fminsearch** command, which uses a simplex search routine. Information on the algorithm can be found in MATLAB documentation. The original algorithm was developed by Nelder and Mead in [88], see also [89] for more recent work.

One issue that arises in the minimization is that the objective function is not necessarily convex, and so there is no guarantee of finding the true minimizer. This means that the parameter estimation is sensitive to the choice of initial conditions (see [90]). To mitigate this problem when calibrating the variance gamma process, we minimize from several different initial points. This strategy is effective for the variance gamma process because we can compute option prices extremely efficiently for this model, and so the minimization is fast.

For a Hunt variance gamma process, it is computationally expensive to price options, and so each calibration requires a nontrivial amount of time. This means that the initial point for the minimization routine must be chosen in an intelligent manner. In our calibration, we set $\sigma_1 = \sigma_2 = \sigma_3$, and set this equal to the value of $\sigma$ from the variance gamma calibration. We repeat with $\nu_1, \nu_2$, and $\nu_3$ and $\theta_1, \theta_2$, and $\theta_3$. Note that in this case, the Hunt variance gamma process reduces to a variance gamma process. So we are starting our Hunt variance gamma calibration with the optimal variance gamma process.

The data we use to calibrate our process is S&P 500 futures option closing prices. We use both call and put options. Only options with a minimum bid price above \$0.25 and open interest above 1500 contracts are used in an effort to base our calibration on only liquidly traded contracts. The data is taken from the Wharton

Research Data Services (WRDS) database.

For the variance gamma process, the best fit was computed for every trading day between September 1, 2006 and December 30, 2011, for a total of 1342 days. The Hunt variance gamma process is calibrated approximately once a month during that same time period, for a total of 52 days. A summary of the fit statistics for the Hunt variance gamma process is given in Figure 4.3, and a summary for the variance gamma process is given in Figure 4.4.

We measure the goodness of fit in three different ways in Figures 4.3 and 4.4. The first column gives information about the daily root mean square error (RMSE). The second column gives the average absolute error (AAE), while the third column represents average absolute percent error (AAPE). We note that the reported AAPE has been computed using only the options with prices greater than \$1, to avoid dividing by very small numbers. These quantities are computed in the following way

$$\begin{aligned} \text{RMSE} &= \sqrt{\frac{1}{N}\sum_{i=1}^{N}(O_i - O_i^{\Theta^*})^2} \\ \text{AAE} &= \frac{1}{N}\sum_{i=1}^{N}|O_i - O_i^{\Theta^*}| \\ \text{AAPE} &= \frac{1}{N}\sum_{i=1}^{N}\left|\frac{O_i - O_i^{\Theta^*}}{O_i}\right|. \end{aligned}$$

The last column gives statistics about the number of options fitted on each day (NO).

A sample calibration for a Hunt variance gamma process is shown in Figure 4.5, while a sample variance gamma calibration is shown in Figure 4.6. These

| Fit Statistics of Hunt VG Process | | | | |
|---|---|---|---|---|
| | RMSE | AAE | AAPE* | NO |
| Mean | 1.224 | 0.887 | 0.088 | 217.3 |
| St Dev | 0.724 | 0.546 | 0.040 | 48.0 |
| 5 pctl | 0.429 | 0.313 | 0.039 | 144.8 |
| 10 pctl | 0.534 | 0.387 | 0.045 | 147.4 |
| 25 pctl | 0.805 | 0.593 | 0.062 | 175.0 |
| 50 pctl | 1.029 | 0.729 | 0.079 | 217.0 |
| 75 pctl | 1.450 | 0.987 | 0.101 | 249.0 |
| 90 pctl | 1.982 | 1.489 | 0.134 | 280.2 |
| 95 pctl | 2.538 | 1.928 | 0.155 | 299.4 |

Figure 4.3: This table shows the fit statistics for a Hunt variance gamma process. A Hunt variance gamma process was fit to option data on 52 trading days evenly spaced between September 1, 2006 and December 30, 2011. This table summarizes the error between model and market prices.

| Fit Statistics of a Variance Gamma Process | | | | |
|---|---|---|---|---|
| | RMSE | AAE | AAPE* | NO |
| Mean | 4.026 | 3.190 | 0.324 | 219.1 |
| St Dev | 2.328 | 1.852 | 0.111 | 49.9 |
| 5 pctl | 1.876 | 1.529 | 0.169 | 144.0 |
| 10 pctl | 2.148 | 1.750 | 0.197 | 154.2 |
| 25 pctl | 2.724 | 2.180 | 0.243 | 179.0 |
| 50 pctl | 3.254 | 2.614 | 0.305 | 217.0 |
| 75 pctl | 4.381 | 3.338 | 0.390 | 257.0 |
| 90 pctl | 7.012 | 5.528 | 0.473 | 288.0 |
| 95 pctl | 8.783 | 6.970 | 0.520 | 301.0 |

Figure 4.4: This table shows the fit statistics for a variance gamma process. A variance gamma process was fit to option data on the 1342 trading days between September 1, 2006 and December 30, 2011. This table summarizes the error between model and market prices.

samples both come from September 1, 2006, the first day on which both models were calibrated. In both cases, the number of options used (NO) was 142. For comparison with the reported fit statistics given in Figures 4.3 and 4.4, we show the fit statistics on this day below. For the Hunt variance gamma calibration,

$$\begin{aligned} \text{RMSE} &= 0.429 \\ \text{AAE} &= 0.335 \\ \text{AAPE} &= 0.051. \end{aligned}$$

The variance gamma calibration had the following fit stats on September 1, 2006

$$\begin{aligned} \text{RMSE} &= 2.134 \\ \text{AAE} &= 1.833 \\ \text{AAPE} &= 0.247. \end{aligned}$$

These fit statistics rank roughly between the 5th and 25th percentile for their respective models, making this an example of a good fit for each model.

We can observe one important distinction between the two models in these images. It was mentioned in the introduction that Lévy processes (which include the variance gamma process) do a poor job of fitting the option surface at multiple maturities. We see evidence of this in Figure 4.6. We see that the variance gamma model overestimates option prices at short maturities (which correspond to lower prices in the image), while underestimating option pricing at longer maturities. The Hunt variance gamma process is much more accurate for multiple maturities.

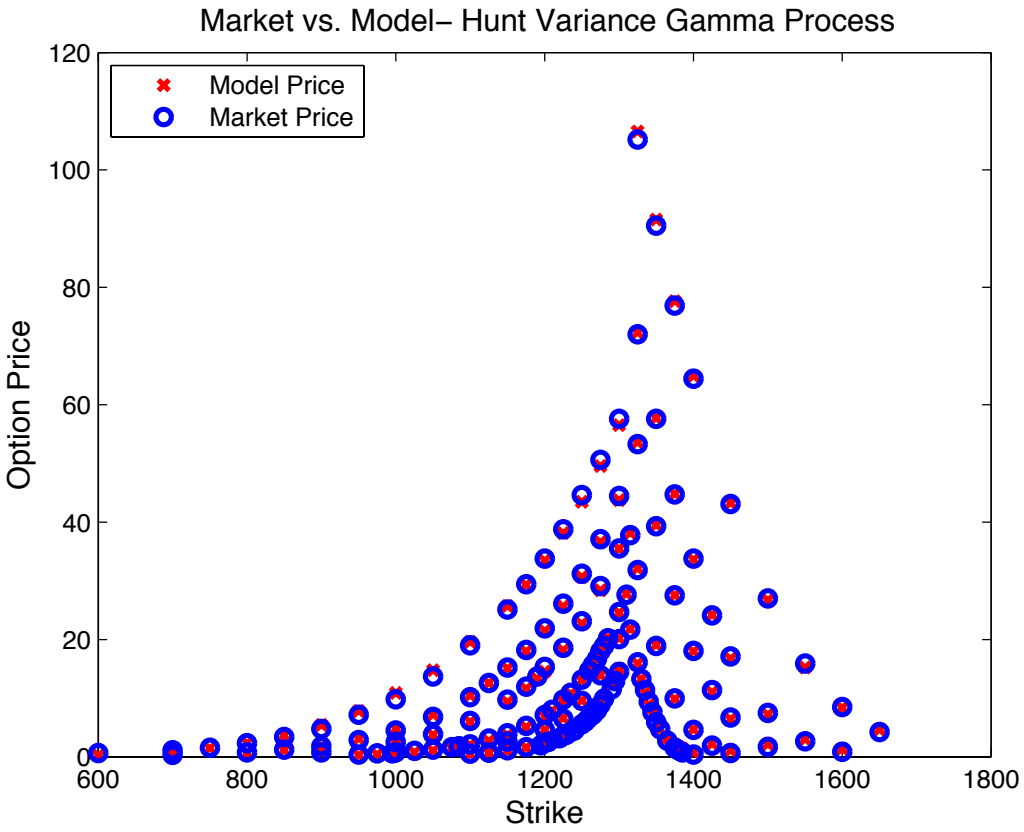


Figure 4.5: This figure shows model prices and market prices for S&P 500 futures options. The model was taken to be a Hunt variance gamma process with parameters chosen to minimize the error between the market and model prices. Option data comes from September 1, 2006. Compare this image with Image 4.6.

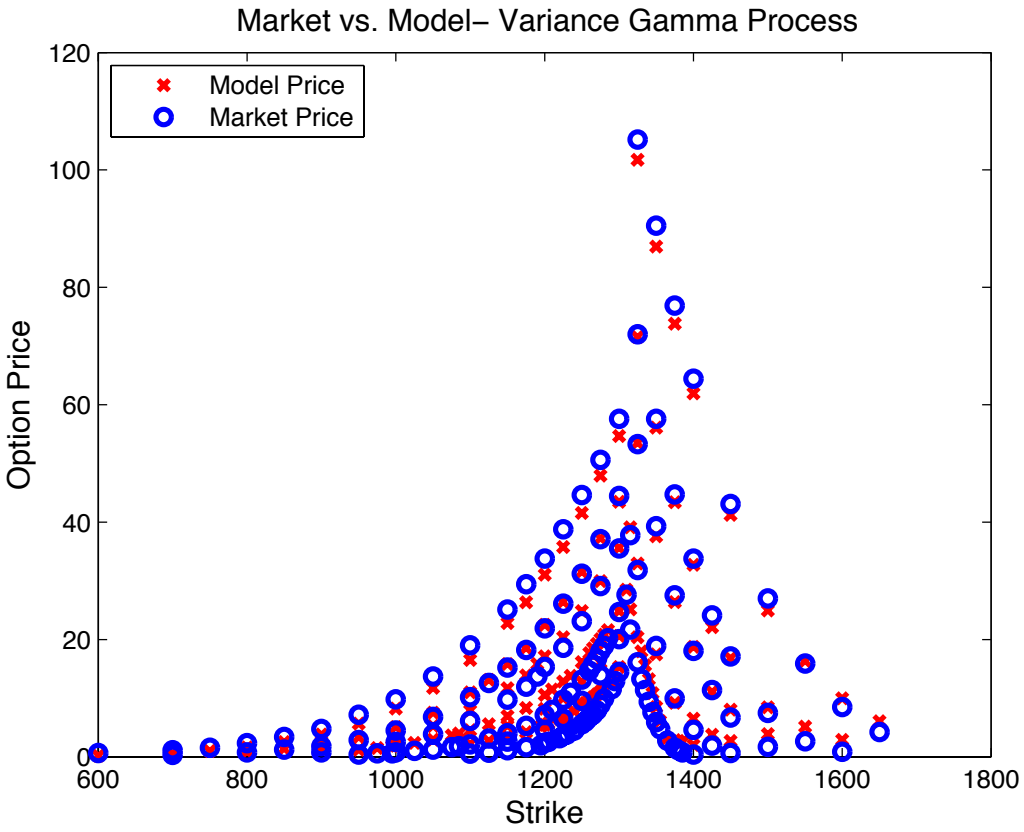


Figure 4.6: This figure shows model prices and market prices for S&P 500 futures options. The model was taken to be a variance gamma process with parameters chosen to minimize the error between the market and model prices. Option data comes from September 1, 2006. Compare this image with Image 4.5.

# Chapter 5

# Characteristics and Applications of the Hunt Variance Gamma Process

In this chapter we investigate several different aspects of the Hunt variance gamma process. We first verify that the process is fundamentally different from both a Lévy process and a Sato process by investigating the marginal distributions at a single time and the evolution of moments over time. Next we investigate how well the term structure of moments matches the market term structure, computed in a model-independent manner.

We then turn our attention to investigating conditional probabilities of certain events, where we condition on the level of the underlying stock. This type of investigation is impossible using a spatially homogeneous model, and so a spatially inhomogeneous model such as the Hunt variance gamma process is required.

## 5.1 Relation to Lévy and Sato Processes

Generally both Lévy and Sato processes are described through either their characteristic exponent or Lévy measure (see [26] for examples). To define the Hunt variance gamma process, we started with the infinitesimal generator and found a solution to the martingale problem. In this section we will show that the resulting process is not a Lévy process, nor is it a Sato process.

This is not an unexpected result. The Hunt variance gamma process was designed so that increments $X_t - X_s$ are not independent of the sigma–algebra $\mathscr{F}_s$, but instead are Markovian. This differs from both the Lévy and Sato process.

### 5.1.1 Time Evolution of Moments

We will first examine the evolution in time of the moments of a Lévy process, and compare this to that of the Hunt VG process. In the discussion below, we will assume that the Lévy process in question has a finite moment generating function, i.e. that $\mathbb{E}[e^{uX_t}] < \infty$. Kruglov gives several criteria for this to occur, see [91]. Also note that for many financial applications, some variant of $e^{X_t}$ is used to model the price of a security, and so a finite moment generating function is standard.

As usual, we let $X_t$ denote a Lévy process, and let its moment generating function be denoted $\mathbb{E}[e^{uX_t}] = \Psi_t(u)$. Observe that if this function exists, the characteristic function of a Lévy process described in Theorem 2.1.4 can be analytically extended to describe it. One important result of this is that if we let $\Psi(u) = \Psi_1(u)$ then

$$\Psi_t(u) = \Psi(u)^t. \tag{5.1}$$

We now follow the process shown in [28] to observe the evolution in time of moments. Standard probability theory tells us that $\mathbb{E}[X_t^j] = \Psi_t^{(j)}(0)$. By differentiating equation (5.1), we can write the moments of $X_t$ in terms of $t$ and the derivatives of $\Psi(u)$.

Let $\Psi_j = \Psi^{(j)}(0)$, the $j$-th derivative of $\Psi(u)$ evaluated at 0. Upon differenti-

ating, we get the following results:

$$\begin{aligned}
\mathbb{E}[X_t] &= t\Psi_1 \\
\mathbb{E}[X_t^2] &= t(t-1)\Psi_1^2 + t\Psi_2 \\
\mathbb{E}[X_t^3] &= t\Psi_3 + t(t-1)(t-2)\Psi_1^3 + 3t(t-1)\Psi_1\Psi_2 \\
\mathbb{E}[X_t^4] &= 6t(t-1)(t-2)\Psi_1^2\Psi_2 + 3t(t-1)\Psi_2^2 + 4t(t-1)\Psi_1\Psi_3 \\
&\quad + t\Psi_4 + t(t-1)(t-2)(t-3)\Psi_1^4.
\end{aligned}$$

Using these equations, we find the moments about the mean

$$\begin{aligned}
\mathbb{E}[(X_t - \mathbb{E}[X_t])^2] &= t(\Psi_2 - \Psi_1^2) \\
\mathbb{E}[(X_t - \mathbb{E}[X_t])^3] &= t(\Psi_3 + 2\Psi_1^3 - 3\Psi_1\Psi_2) \\
\mathbb{E}[(X_t - \mathbb{E}[X_t])^4] &= 3t^2(\Psi_2 - \Psi_1^2) + t(12\Psi_1^2\Psi_2 - 3\Psi_2^2 - 4\Psi_1\Psi_3 + \Psi_4 - 6\Psi_1^4).
\end{aligned}$$

Finally, we see that the skewness of $X_t$ is given by

$$\frac{\mathbb{E}[(X_t - \mathbb{E}[X_t])^3]}{\mathbb{E}[(X_t - \mathbb{E}[X_t])^2]^{3/2}} = \frac{1}{\sqrt{t}}\left(\frac{\Psi_3 + 2\Psi_1^3 - 3\Psi_1\Psi_2}{(\Psi_2 - \Psi_1^2)^{3/2}}\right),$$

and the excess kurtosis of $X_t$ is

$$\frac{\mathbb{E}[(X_t - \mathbb{E}[X_t])^4]}{\mathbb{E}[(X_t - \mathbb{E}[X_t])^2]^2} - 3 = \frac{1}{t}\left(\frac{12\Psi_1^2\Psi_2 - 3\Psi_2^2 - 4\Psi_1\Psi_3 + \Psi_4 - 6\Psi_1^4}{(\Psi_2 - \Psi_1^2)^2}\right).$$

We can use these results to test to see if the Hunt Variance Gamma process is a Lévy process. If so, the skewness and excess kurtosis will decline at a rate proportional to $1/\sqrt{t}$ and $1/t$, respectively. To do so, we construct a Markov chain approximation to any Hunt VG process using the ideas from Chapter 4, and then calculate the skewness and excess kurtosis at several different times, and observe the decay.

We did this for Hunt VG processes using several different parameters, and found that the skewness and excess kurtosis did not decay proportional to $1/\sqrt{t}$ and $1/t$. To control for error introduced by the approximation scheme, we approximated known Lévy processes (in this case, a variance gamma process) using the same scheme, and found the expected decay. These experiments showed that the Hunt VG process does not satisfy a basic characteristic of Lévy processes, and is thus not a Lévy process.

Sample results of these experiments are given in Figure 5.1 and Figure 5.2. Figure 5.1 shows skewness $\times \sqrt{t}$ for a Hunt VG process (approximated using methods from Chapter 4), a VG process (also approximated), and the true value for the same variance gamma process. Figure 5.2 shows (kurtosis $- 3$) $\times\, t$ for the same three processes. One can see in the figures that the Markov Chain approximation method gives a result that is essentially constant in both cases, but that the Hunt VG process is decidedly not.

### 5.1.2 Non-Infinite Divisibility of Marginal Distributions

Next we examine a marginal distribution of the Hunt Variance Gamma process and compare it to that of an infinitely divisible distribution. Recall that the predominant feature of a Lévy process, as discussed in Section 2.1, is that the law of a Lévy process is infinitely divisible. The same is true of Sato processes. This fact allowed us to use the Lévy-Khintchine representation to describe the characteristic function of both Lévy and Sato processes. We now show that the distribution of a

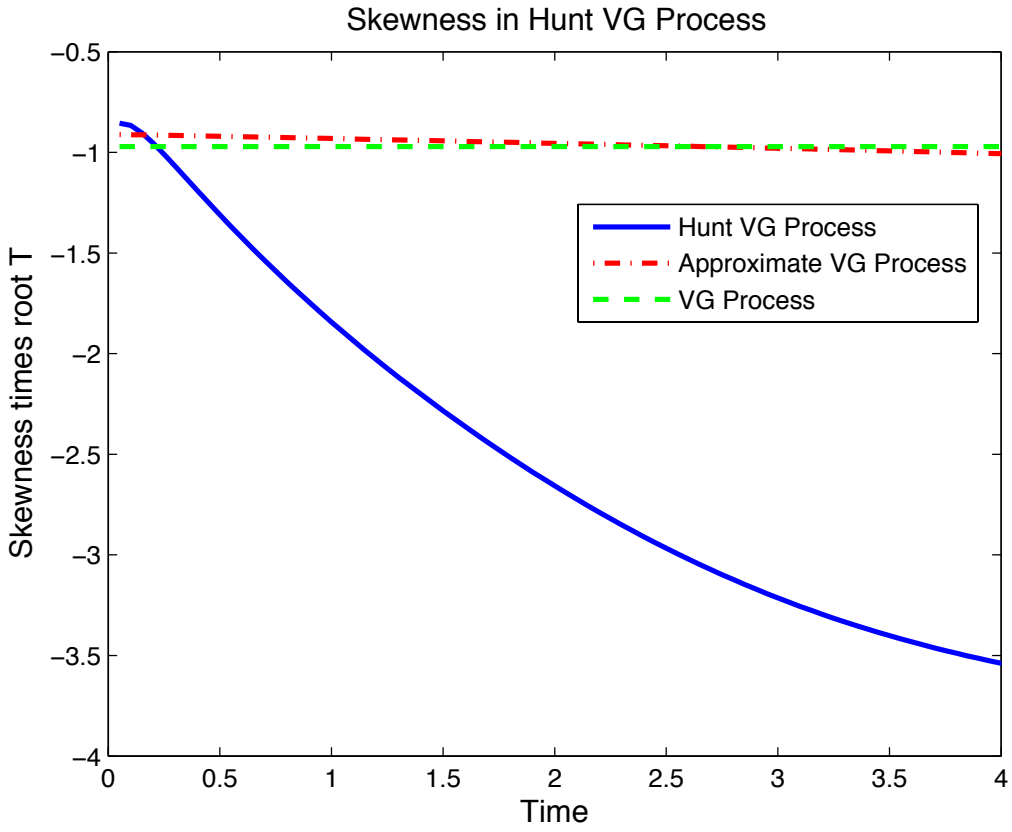


Figure 5.1: This figure shows the skewness in time of two processes. One is a Hunt Variance Gamma process with parameters $\sigma_1 = 0.458$, $\nu_1 = 0.128$, $\theta_1 = 0.746$, $\sigma_2 = 0.149$, $\nu_2 = 0.251$, $\theta_2 = -0.484$, $\sigma_3 = 0.106$, $\nu_3 = 0.001$, and $\theta_3 = 0.135$. The other process is a variance gamma process with parameters $\sigma = 0.149$, $\nu = 0.251$, and $\theta = -0.484$. The skewness of this process is computed in two ways, one using the exact number and the other using the Markov Chain approximation method detailed in Chapter 4.

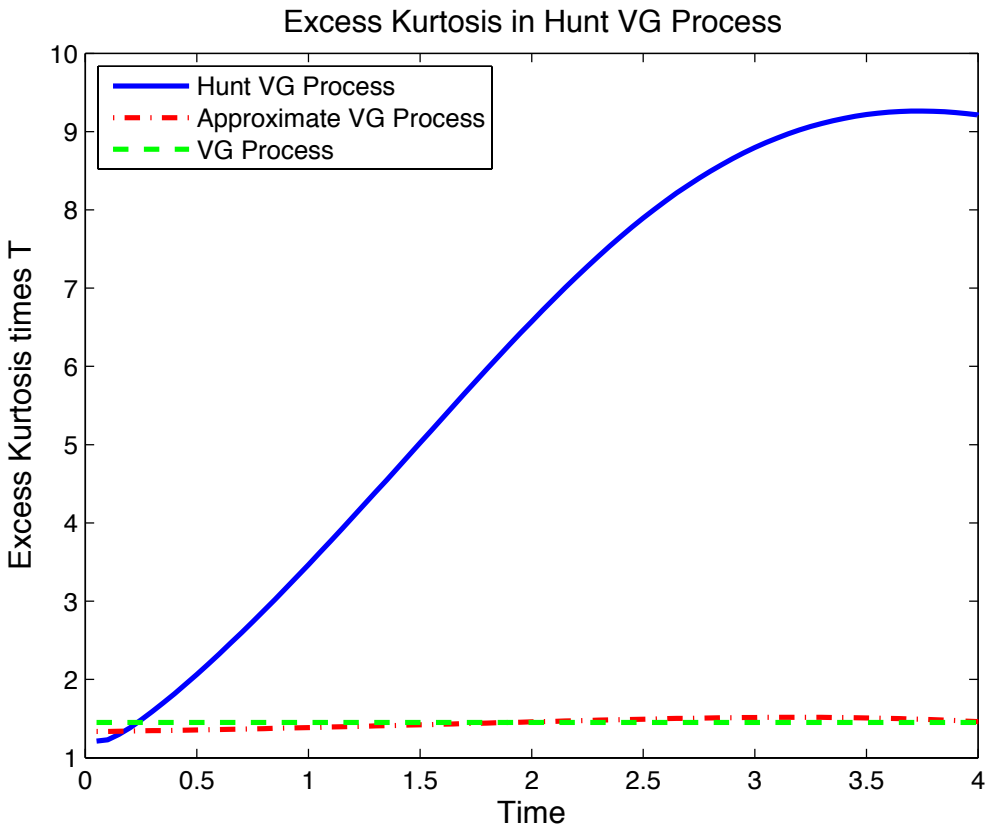


Figure 5.2: This figure shows the excess kurtosis in time of the same two process detailed in Figure 5.1.

Hunt Variance Gamma process is not infinitely divisible.

In order to do this testing, we will use several ideas from Fourier analysis. The Fourier transform of an integrable function $f$, denoted by $\hat{f}$, is given by

$$\hat{f}(u) = \int_{-\infty}^{\infty} e^{iux} f(x) dx.$$

We also define the inverse Fourier transform, which, when applied to an integrable function $\hat{f}(u)$ gives

$$f(x) = \frac{1}{2\pi} \int_{-\infty}^{\infty} e^{-iux} \hat{f}(u) du.$$

As the name and notation suggest, there is a relationship between the Fourier transform and inverse Fourier transform, developed by Plancherel in [92] and [93]. This theorem tells us that the Fourier transform defined above can be extended to a linear bijection between functions in $L^2(\mathbb{R})$. We do not need to go into this much detail, and instead use a weaker version, the Jordan Theorem. A proof of this theorem is given in [94].

**Theorem 5.1.1** (Jordan)**.** *Suppose that $f$ is a continuous, integrable function of bounded variation. Let $\hat{f}(u)$ denote the Fourier transform of $f$. Then*

$$f(x) = \lim_{a \to \infty} \frac{1}{2\pi} \int_{-a}^{a} e^{-ixu} \hat{f}(u) du$$

With this information in hand, we are prepared to demonstrate that the law of the Hunt VG process is not infinitely divisible. To do so, recall the Lévy-Khintchine theorem, first shown in Theorem 2.1.4. It says

**Theorem 5.1.2** (Lévy-Khintchine)**.** *The characteristic function of any Lévy process*

*$X_t$ can be written as*

$$\mathbb{E}[e^{iuX_t}] = e^{t\psi(u)},$$

*where*

$$\psi(u) = i\mu u - \frac{1}{2}\sigma^2 u^2 + \int_{\mathbb{R}} \left(e^{iux} - 1 - iux\mathbf{1}_{\{|x|<1\}}\right) \Pi(dx)$$

*and* $\int (1 \wedge x^2)\Pi(dx) < \infty$. *Here* $\psi(u) = log(\mathbb{E}[e^{iuX_1}])$.

Observe that if there is no Brownian component to the Lévy process, then

$$\psi''(u) = -\int_{\mathbb{R}} x^2 e^{iux} \Pi(dx).$$

We see that for a Lévy process, the second derivative of the characteristic exponent is the Fourier transform of $x^2\Pi(dx)$, the Lévy measure. If we assume that the Lévy measure $\Pi$ is absolutely continuous with respect to Lebesgue measure, and furthermore that it is continuos and has bounded variation, we can apply the Jordan Theorem to recover $x^2\Pi(x)$. In this case

$$x^2\Pi(x) = -\frac{1}{2\pi}\int_{-\infty}^{\infty} \psi''(u)e^{-iux}du. \tag{5.2}$$

In [21] it is argued that infinite activity models are a suitable substitute for models which include a Brownian component, so we are unconcerned about the assumption that no Brownian component is present. In fact, several papers have argued that models with infinitely many small jumps give a better representation of asset behavior than Brownian motion can (see [95]). The other assumptions are satisfied by almost every common Lévy process used in financial mathematics (every example in [26] except for a Poisson process satisfies this criteria).

In Chapter 4, we developed an algorithm to approximate the Hunt VG process. Using this approximation, we can compute an approximation to

$$\psi(u) = \log\left(\mathbb{E}[e^{iuX_t}]\right).$$

To show that the distribution of $X_t$ is not necessarily infinitely divisible, we can compute $x^2\Pi(x)$ using equation (5.2), and show that $\Pi(x)$ is not always positive. Note that for a Lévy process, it must be.

Rather than do the computation from equation (5.2) directly, we use another fact from Fourier analysis, namely that there is a relationship between the inverse Fourier transform of a derivative and the inverse transform of the original function. This relationship can be seen by integrating equation (5.2) by parts twice. Then

$$x^2\Pi(x) = -\frac{x^2}{2\pi}\int_{-\infty}^{\infty}\psi(u)e^{-iux}du.$$

To perform this integration, we begin by choosing a value $M$ and perform the integration between $-M$ and $M$. Then

$$x^2\Pi(x) \approx -\frac{x^2}{2\pi}\int_{-M}^{M}\psi(u)e^{-iux}du. \tag{5.3}$$

This step has an impact on the accuracy of our results, which we will discuss later.

We also choose $N$, the number of steps we will use to perform the integration. We partition the real line along the points $u_j$ stretching between $-M$ and $M$, by letting

$$u_j = -M + (j-1)\frac{2M}{N} \text{ for } j = 1, \ldots, N.$$

Set $\psi_j = \psi(u_j)$. Using this notation, we can approximate equation (5.3) by

$$x^2\Pi(x) \approx -\frac{x^2}{2\pi}\sum_{j=1}^{N}\psi_j e^{-iu_j x}\frac{2M}{N}.$$

This integration can be performed more efficiently using the Fast Fourier Transform (see [96] for a history of the development). This is done by setting $\lambda = \pi/M$, $b = \frac{\pi N}{2M}$, and $x_u = -b + \lambda(u-1)$ for $u = 1, \ldots, N$. Then we see that

$$x_u^2 \Pi(x_u) = -\frac{M}{\pi N} x_u^2 e^{iMx_u} \sum_{j=1}^{N} \psi_j e^{ib\frac{2M}{N}(j-1)} \left(e^{-\frac{2\pi i}{N}}\right)^{(j-1)(u-1)}.$$

This sum can be evaluated for all $N$ values of $x_u$ in time $N \log_2(N)$ instead of $N^2$ using an algorithm developed by Cooley and Tukey in [97]. The MATLAB command **fft** can be used for this purpose.

There is error in the computation involved, particularly for small values of $x$. For this reason, it will be convenient to solve for $x\Pi(x)$. This gives the equation we will use for computation, which is

$$x_u \Pi(x_u) = -\frac{M}{\pi N} x_u e^{iMx_u} \sum_{j=1}^{N} \psi_j e^{ib\frac{2M}{N}(j-1)} \left(e^{-\frac{2\pi i}{N}}\right)^{(j-1)(u-1)}. \tag{5.4}$$

Figure 5.3 shows a sample of the results of this integration for a Hunt VG process. Observe that in this image, there is a section where $x\Pi(x) < 0$ for positive $x$, showing that the law of the Hunt VG process is not infinitely divisible. This result can be compared to the result obtained by applying this procedure to a variance gamma process obtained using the same methodology. The result is given in Figure 5.4, together with the true value obtained using equation (3.3).

One feature of these figures is that the computed Lévy measure appears to oscillate. The cause of this oscillation is the decision to truncate the integration outside of the set $[-M, M]$. We explain this principle below.

To understand, we first define a convolution. For two integrable functions $f$

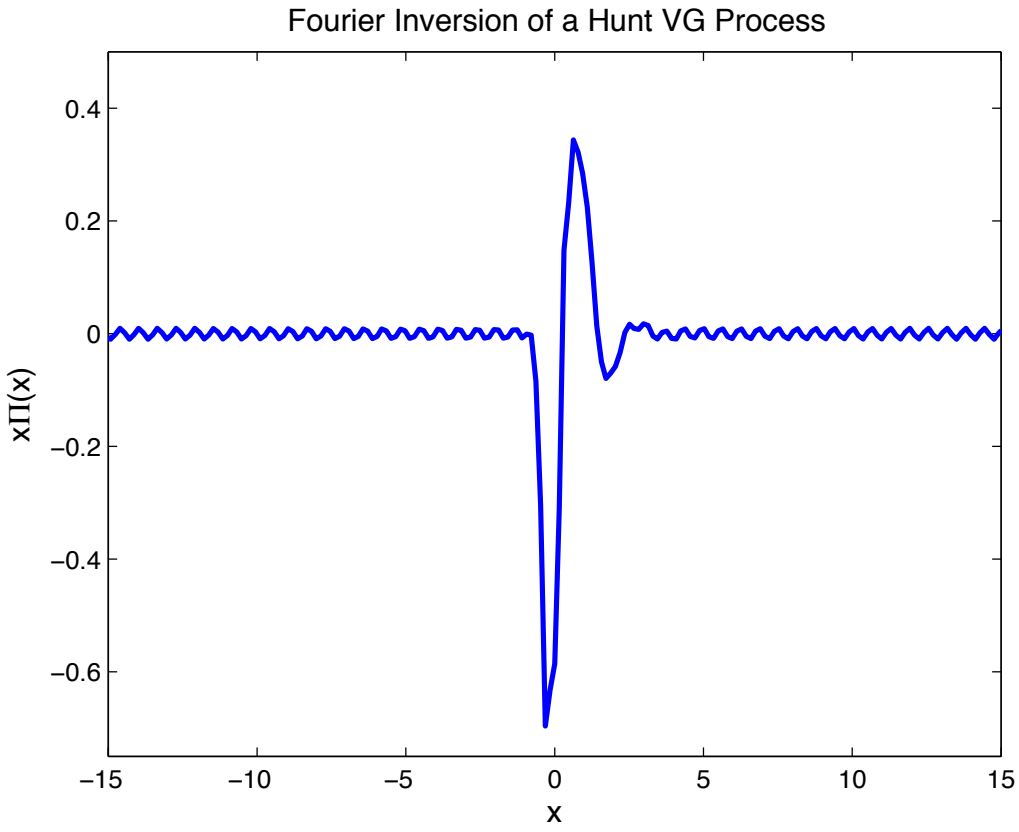


Figure 5.3: This figure shows the result of applying equation (5.4) to a Hunt VG process with parameters $\sigma_1 = 0.3$, $\nu_1 = 0.1$, $\theta_1 = -0.1$, $\sigma_2 = 0.3$, $\nu_2 = 0.1$, $\theta_2 = 0.5$, $\sigma_3 = 0.3$, $\nu_3 = 0.1$, and $\theta_3 = -0.1$.

For the integration settings we use $N = 2^{12}$ and $M = 20$.

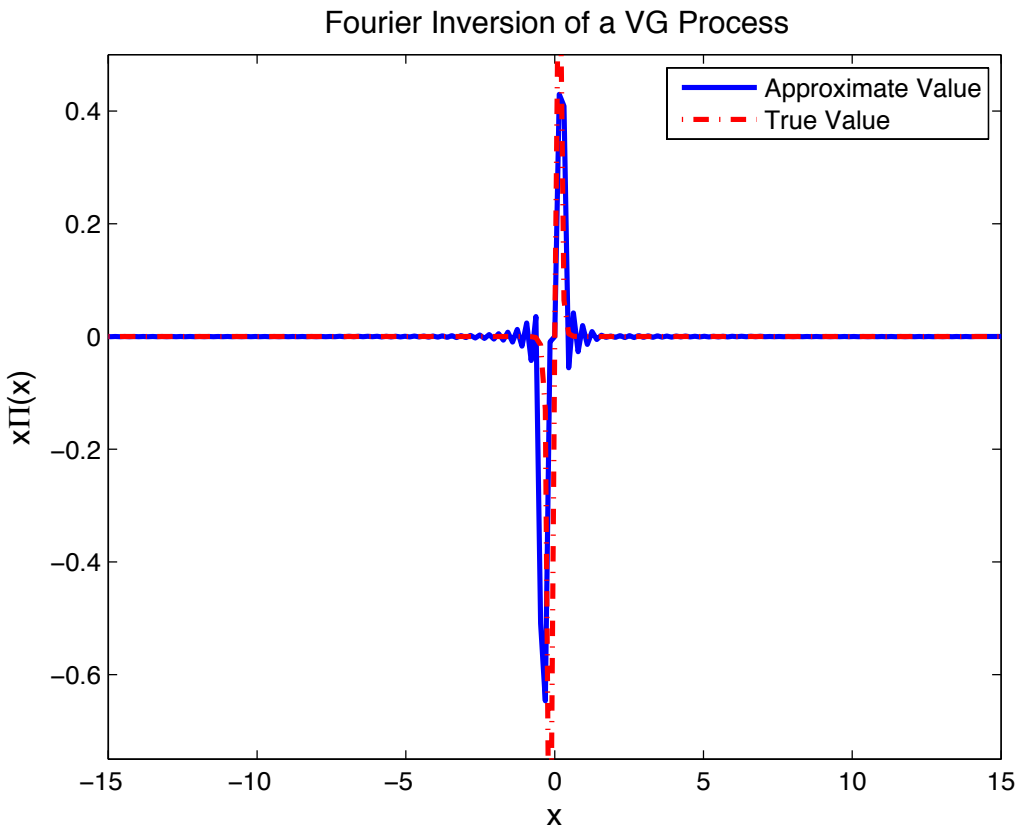


Figure 5.4: This figure shows the result of applying equation (5.4) to a VG process with parameters $\sigma = 0.3$, $\nu = 0.1$, and $\theta = -0.1$. The true Lévy measure is shown together with the approximation using the same method as in Figure 5.3.

and $g$, the convolution of $f$ with $g$, denoted $f * g$, is given by

$$f * g(u) = \int_{-\infty}^{\infty} f(u-x)g(x)dx.$$

The Fourier transform has the interesting property that it converts convolutions to products and products to convolutions (see [94]). In other words, if $f$ has Fourier transform $\hat{f}$, and $g$ has Fourier transform $\hat{g}$, then

$$\widehat{f * g} = \hat{f}\hat{g}.$$

With this in mind, we rewrite equation (5.3) as

$$-\frac{x}{2\pi}\int_{-M}^{M}\psi(u)e^{-iux}du = -\frac{x}{2\pi}\int_{-\infty}^{\infty}\psi(u)\mathbf{1}_{\{|u|<M\}}e^{-iux}du,$$

so that we are taking the inverse Fourier transform of a product. We can see from the property above that our result, instead of being the true inverse Fourier transform ( which is $x\Pi(x)$ ), will be the convolution of $x\Pi(x)$ with the inverse Fourier transform of the indicator function $\mathbf{1}_{\{|x|<M\}}$.

This function can be found by direct computation, as

$$\frac{1}{2\pi}\int_{-\infty}^{\infty}\mathbf{1}_{\{|u|<M\}}e^{-iux}du = \frac{1}{2\pi}\int_{-M}^{M}e^{-iux} = \frac{1}{\pi x}\sin(Mx).$$

This is related to the well known sinc function.

We have shown that the procedure detailed above to compute $x\Pi(x)$ is actually approximating

$$x\Pi(x) * \frac{1}{\pi x}\sin(Mx).$$

This accounts for the oscillation seen in Figures 5.3 and 5.4.

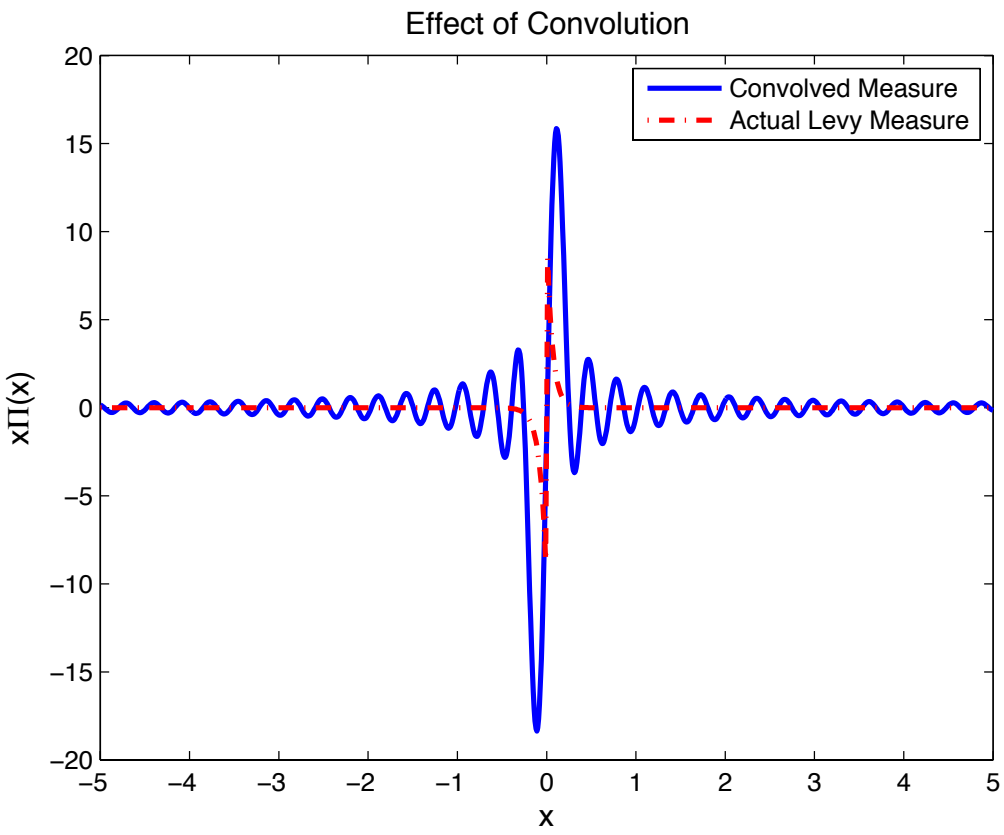


Figure 5.5: This figure shows the effect of convolution with a sinc function on the function $x\Pi(x)$. Here we use a variance gamma process. The introduction of oscillation can clearly be seen.

We show the impact of this oscillation in Figure 5.5. Here we see the actual value of $x\Pi(x)$ for a variance gamma process, which is shown in equation (3.3), together with the convolution of this measure with $\frac{1}{\pi x}\sin(Mx)$. Observe that after convolution, oscillation is introduced into the Lévy measure.

In this section, we have shown that the distribution of a Hunt variance gamma process is not infinitely divisible, which means that the law given by a Hunt variance gamma process cannot come from a Lévy process. For additive processes such as the

Sato process described in the introduction, the distribution is also infinitely divisible at every time (see [42]). This means that the Hunt variance gamma processes is also not an additive process. Both Lévy processes and Sato processes are spatially homogeneous, so this is an expected result.

## 5.2 Term Structure of Marginal Distributions

In Section 5.1.1, we showed that the scaled moments of the Hunt variance gamma process are not constant. In this section, we investigate how well these match the market evolution of risk neutral moments.

It is well known that we can find the risk neutral distribution of a stock from option prices in the market. Denote the risk neutral density of the stock at time $T$ by $f_T(x)$. Let $C(T,K)$ be the current price of a call option with strike $K$ and expiration $T$, which is observable in the market. The relationship between $f$ and $C$ is given by

$$C(T,K) = \int_K^\infty (S-K)^+ f_T(x)dx.$$

Dupire showed in [8] that we can recover the risk neutral density $f_T$ by setting

$$f_T(K) = \frac{\partial^2 C}{\partial K^2}(K,T).$$

We would like to analyze the relationship between the marginal risk neutral densities observed in the market and the risk neutral densities obtained from the model. Before looking at these full distributions though, we will start by analyzing the moments of these distributions, and specifically how they evolve in time.

To find moments from the market, we use work in [29] and [30]. These papers develop a method to price European options with any twice-continuously differentiable payoff function, $H(S_T)$. They show that for any terminal value $S_T$,

$$\begin{aligned} H(S_T) &= H(S_0) + (S_T - S_0)H_x(S_0) + \int_{S_0}^{\infty} H_{xx}(K)(S_T - K)^+ \, dK \\ &\quad + \int_0^{S_0} H_{xx}(K)(K - S_T)^+ \, dK. \end{aligned}$$

By taking risk neutral expectations of both sides, we get the risk neutral price of a hypothetical claim $e^{-rT}\mathbb{E}[H(S_T)]$ in terms of a portfolio of stock, bonds, and out of the money put and call options. We see that

$$\begin{aligned} e^{-rT}\mathbb{E}[H(S_T)] &= \left(H(S_0) - S_0 H_x(S_0)\right) e^{-rT} + H_x(S_0)S_0 \\ &\quad + \int_{S_0}^{\infty} H_{xx}(K)C(T,K) \, dK + \int_0^{S_0} H_{xx}(K)P(T,K) \, dK. \end{aligned}$$

We can use these equations to find the price of three contracts, which are referred to as the volatility contract, the cubic contract, and the quartic contract in [29]. If we set $R_T = \log(S_T) - \log(S_0)$, these contracts are given by the function

$$H(S_T) = \begin{cases} R_T^2 & \text{Volatility Contract} \\ R_T^3 & \text{Cubic Contract} \\ R_T^4 & \text{Quartic Contract} \end{cases}.$$

Finally, using the prices of these contracts, it is a straightforward to find the risk neutral return volatility, skewness, and excess kurtosis. As mentioned earlier, these quantities are computed from the market in a model-free way.

We compare the market evolution of moments to the moments generated by the Hunt variance gamma process. The model return volatility, skewness, and excess

kurtosis are computed the same way they were in Section 5.1.1. As we did there, we will scale volatility by $\frac{1}{\sqrt{t}}$, skewness by $\sqrt{t}$, and kurtosis by $t$.

A sample plot of the time evolution of volatility, skewness, and kurtosis is shown in Figure 5.6 for the market moments and Hunt process moments. We recall that in Section 5.1.1, we showed that the term structure evolution for a Lévy process is flat, and so a Lévy process will not capture the evolution seen in Figure 5.6. We can also see in this image that the Hunt variance process does a reasonable job of fitting the overall shape of this evolution, although the actual values are not an exact match.

We summarize the shape of the market and model term structure of moments by finding volatility, skewness, and excess kurtosis at 3 months, 6 months, and 9 months. Using these three points, we compute the first and second derivative with respect to time of the moment in question. We can then compare market and model via these derivatives. We do this for all 52 days for which the Hunt variance gamma process was calibrated (see Section 4.3). A summary of the absolute error is shown in Figure 5.7.

We see from this table that the Hunt variance gamma process fits the general shape of the market moments in a reasonable way, although the fit itself is far from perfect. A better way of summarizing this information is to compare the sign of each model derivative with its corresponding market derivative. There are six total derivatives to compare (two each for volatility, skewness, and kurtosis), and if the signs for all six match up than we have correctly approximated the shape of the term structure of the moments. A summary of the 52 calibrated days is given below.

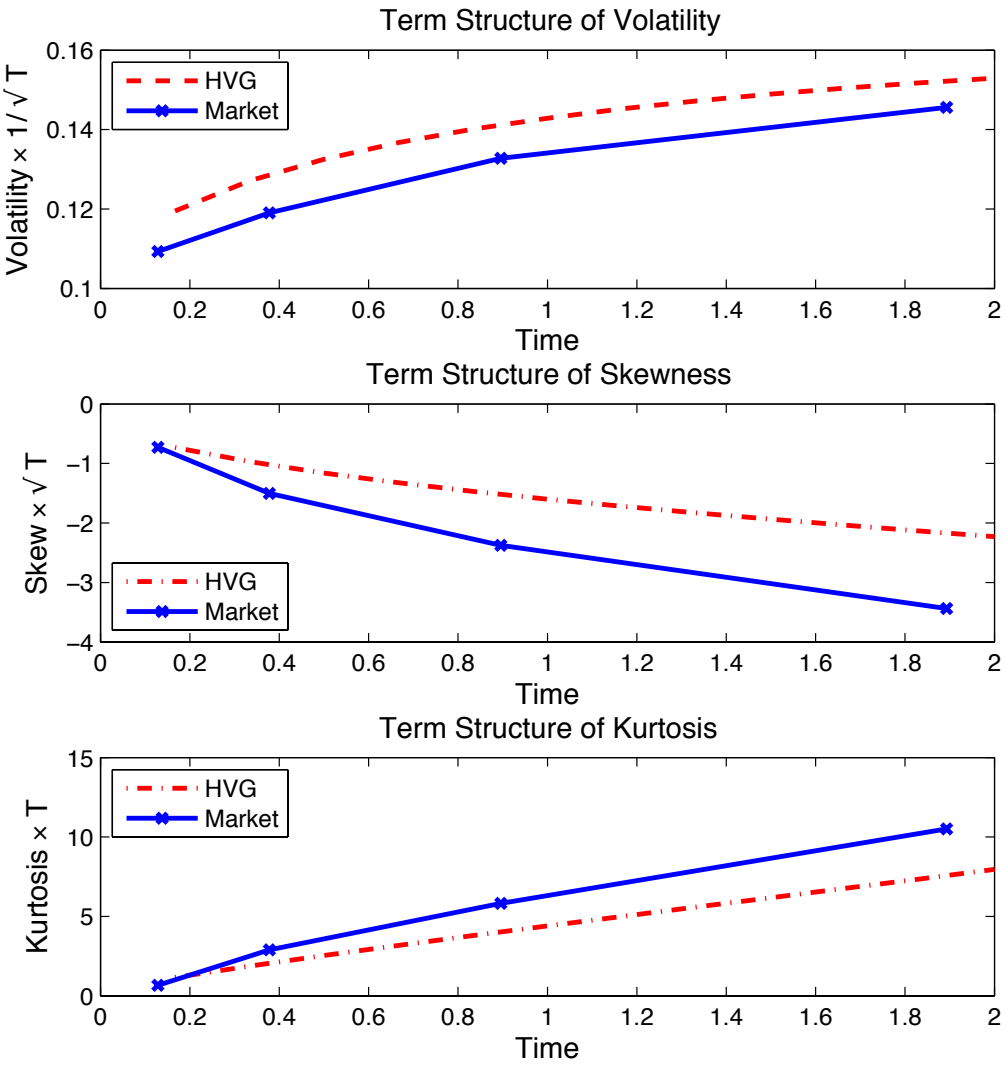


Figure 5.6: This figure shows the scaled volatility, skewness, and kurtosis calculated from the market and compares it to the same scaled moments taken from a calibrated Hunt variance gamma process. The market data and calibration come from January 29, 2007.

| Absolute Error | | | | | | |
|---|---|---|---|---|---|---|
| | $\frac{\partial}{\partial t}$ vol | $\frac{\partial^2}{\partial t^2}$ vol | $\frac{\partial}{\partial t}$ skew | $\frac{\partial^2}{\partial t^2}$ skew | $\frac{\partial}{\partial t}$ kurt | $\frac{\partial^2}{\partial t^2}$ kurt |
| Mean | 0.031 | 0.142 | 0.647 | 2.913 | 2.741 | 8.671 |
| St Dev | 0.034 | 0.143 | 0.403 | 2.715 | 1.652 | 7.494 |
| 5 pctl | 0.002 | 0.014 | 0.080 | 0.056 | 0.263 | 1.035 |
| 10 pctl | 0.004 | 0.021 | 0.156 | 0.246 | 0.406 | 1.208 |
| 25 pctl | 0.010 | 0.046 | 0.375 | 0.748 | 1.176 | 3.222 |
| 50 pctl | 0.018 | 0.089 | 0.606 | 1.800 | 2.556 | 6.060 |
| 75 pctl | 0.038 | 0.189 | 0.811 | 4.053 | 3.953 | 13.640 |
| 90 pctl | 0.065 | 0.294 | 1.146 | 7.260 | 4.813 | 19.768 |
| 95 pctl | 0.086 | 0.390 | 1.337 | 7.941 | 5.377 | 23.022 |

Figure 5.7: This table shows the average absolute error between the derivatives of the market and model scaled moments. As a reference, the market absolute average for each of the columns above is $\frac{\partial}{\partial t}$ vol $= 0.058$, $\frac{\partial^2}{\partial t^2}$ vol $= 0.161$, $\frac{\partial}{\partial t}$ skew $= 1.62$, $\frac{\partial^2}{\partial t^2}$ skew $= 3.66$, $\frac{\partial}{\partial t}$ kurt $= 2.65$, and $\frac{\partial^2}{\partial t^2}$ skew $= 8.94$.

| Derivatives Missed | 0 | 1 | 2 | 3 | 4 | 5 | 6 |
|---|---|---|---|---|---|---|---|
| # Of Days | 20 | 12 | 15 | 4 | 0 | 1 | 0 |

We observe that the Hunt variance gamma calibration correctly gets the sign of the derivative for the term structure of all 3 moments on just less than 40% of the days. There are two or less errors on more than 90% of the calibrated days. This means that in general, the Hunt variance gamma process accurately reflects the general shape of the market term structure of volatility, skewness, and kurtosis.

## 5.3 Mean Reversion in Conditional Jump Probabilities

One of the important purposes in constructing the Hunt variance gamma process was to develop a process which was truly Markovian instead of just having independent increments. In this section, we investigate how changes to the state of the process affect the risk-neutral distributions. We do this by comparing the probability of large jumps to the probability of a large jump conditional on a large jump already occurring.

Questions of this nature are relevant in the context of financial markets. Large jumps are observed to happen frequently, and so it is of interest to see what the risk neutral probability distribution is conditioning on the occurrence of such an event. Spatially in-homogeneous processes such as the Hunt variance gamma process are one way in which we can investigate these problems.

We first make some simple observations for stock prices driven by processes with independent increments, such as Lévy processes or Brownian motion. Let the

stock price $S_t$ be given by the standard model $S_t = S_0 e^{X_t}$ where $X_t$ has independent increments. Assume that there is immediately a 10% jump up from $S_0$, so that $S_\epsilon = 1.10 S_0$. Then we calculate the probability of a second jump upwards of 10% to be

$$\begin{aligned}
\mathbb{P}\left(S_t > 1.10 S_\epsilon | S_\epsilon = 1.10 S_0\right) &= \mathbb{P}\left(e^{X_t - X_\epsilon} > 1.10 | S_\epsilon = 1.10 S_0\right) \\
&= \mathbb{P}\left(e^{X_t - X_\epsilon} > 1.10\right) \\
&\approx \mathbb{P}(S_t > 1.10 S_0).
\end{aligned}$$

We see that for processes having independent increments, the ratio

$$\frac{\mathbb{P}\left(S_t > 1.10 S_\epsilon | S_\epsilon = 1.10 S_0\right)}{\mathbb{P}(S_t > 1.10 S_0)}$$

is constant and equal to 1. This is true regardless of the size of the move under consideration.

In Figure 5.8, we show a plot of this ratio over time for the Hunt variance gamma process. We also consider

$$\frac{\mathbb{P}\left(S_t < 0.90 S_\epsilon | S_\epsilon = 0.90 S_0\right)}{\mathbb{P}(S_t < 0.90 S_0)},$$

the risk-neutral probability of a large downward jump conditional on a large downward jump.

We make several observations about these results. The first observation is that the ratio plotted in Figure 5.8 is not unity. The probability of a large move conditional on a large move is different from the equivalent probability of a large move. We also can note that the ratio changes in time, reflecting changes to the risk neutral probability distribution.

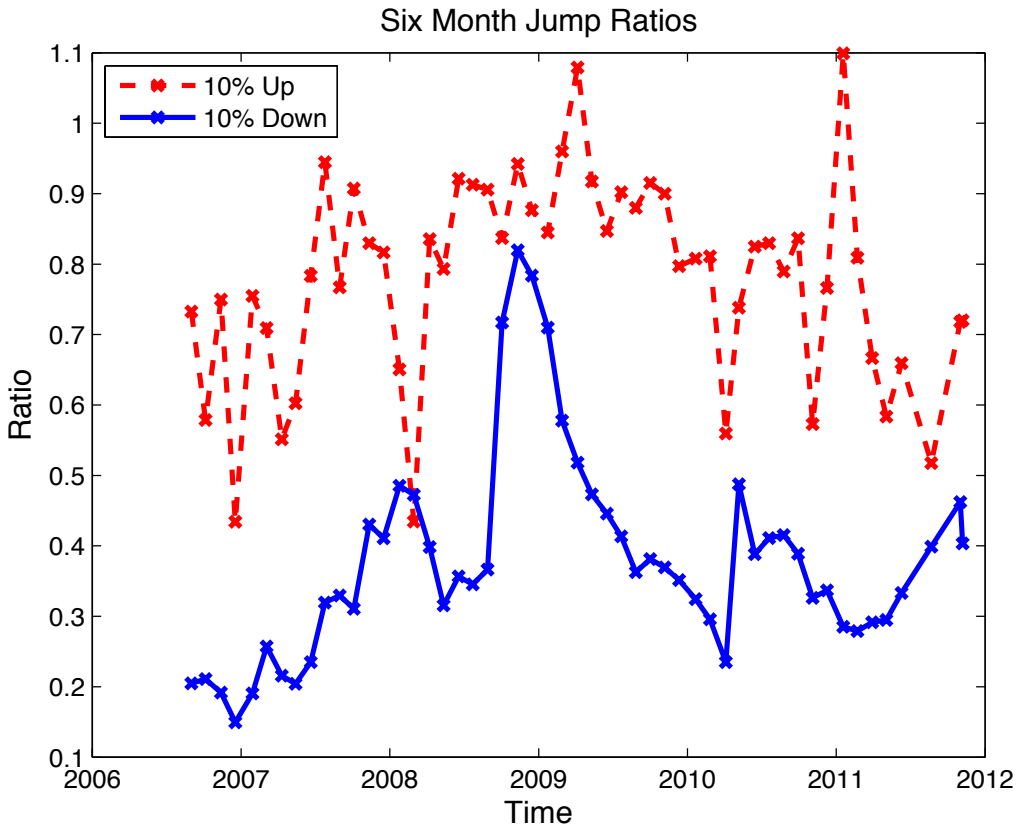


Figure 5.8: This figure shows the probability of a 10% jump in each direction conditional on a previous 10% jump in the same direction, normalized by the probability of a 10% jump. This is done for 52 days between 2006 and 2012.

Another observation is that the ratio in Figure 5.8 is generally less than 1. This indicates that a large jump conditional on a large jump in the same direction is less likely to occur than a large jump in general. We call this mean-reversion, although we remind the reader that $X_t$ is a martingale and so mean-reversion is not possible in its true sense. However in the sense described above, the market is almost always seen to be mean-reverting, particularly when it comes to movemente downward.

We also note that the ratio is much lower for a jump in the downward direction. Further investigation reveals that the denominator for down jumps, $\mathbb{P}(S_t < 0.90S_0)$, is much larger than the denominator of the up jumps, $\mathbb{P}(S_t > 1.10S_0)$, while the numerators are similar in magnitude.

One final item to notice in Figure 5.8 is the large jump in the ratio of 10% downward jumps in late 2008. This period of time was marked by unrest in the global financial markets because of the subprime meltdown. This period started on September 7, 2008 when Fannie Mae and Freddie Mac were taken over by the federal government, and culminated with the bankruptcy of Lehman Brothers on September 15, 2008. The Troubled Asset Relief Program (TARP) was signed into law on October 3, although volatility and large movements in the stock market persisted for weeks and months afterwards. Figure 5.8 shows that the ratio of large downward jumps reached its highest point during this time, and stayed there into early 2009. We assume that the financial crisis changed the behavior of investors for a time, and this is one result.

## 5.4 Conclusions and Further Work

In this dissertation, we have defined a spatially inhomogeneous Markov process which can be used to model stock prices. We shown how to compute probabilities and price options using this process. Using market data, we calibrated this process to the S&P 500 futures prices over five year. We showed that the resulting stochastic process is distinct from both Lévy and Sato processes. Finally, we investigated several characteristics of this process, showing that it more accurately fits the market evolution of moments and investigating the question of conditional probabilities after large jumps.

In the future, we wish to better characterize the impact of each parameter on the process. We currently have very little understanding as to what happens when a parameter gets changed, and because of this, it is difficult to calibrate the process and to draw conclusions once the process has been calibrated. One way of investigating this to consider how the moments change as parameters are changed. Another approach that we are investigating is to compute the reverse conditional expectation function, which for fixed $u < t$ is given by

$$f(S) = \mathbb{E}[S_u | S_t = S].$$

More generally, another avenue that could be explored are different Hunt processes. In this dissertation we have worked exclusively with a Hunt variance gamma process, but the results in Chapter 3 can easily be generalized to create different Hunt processes. For example, we could use more complicated functions for $\sigma$, $\nu$, and $\theta$, or even create an entirely new process based on a different Lévy measure.

This creates another question, namely what is the optimal Hunt process for use. In this setting, the optimal process will depend on its desired use. However, before we can tailor Hunt processes for their intended uses, we need to better understand how spatial inhomogeneity affects the process. A first step would be to understand how each parameter in the Hunt variance gamma process influences the overall process, or at least specific aspects of it. For example, if we understood how changing parameters impact the time evolution of moments, we could choose parameter functions so that they fit the market time evolution of moments.

Finally, we can use the Hunt variance gamma process to gain insight into how the market is pricing different events. We have already investigated the risk-neutral probabilities of large jumps conditioned on large jumps, but this is just an example of what can be done. Economists and empirical financial researchers could use this or similar processes to answer a variety of questions which require a spatially inhomogeneous model.

# Bibliography


[1] Louis Bachelier. Theorie de la speculation. *Ann. Sci. 6c*, 17:21–86, 1900.

[2] Paul H. Cootner. *The Random Character of Stock Market Prices*. MIT Press, 1964.

[3] Fischer Black and Myron Scholes. The Pricing of Options and Corporate Liabilities. *The Journal of Political Economy*, 81(3):637–654, 1973.

[4] Robert C. Merton. Theory of Rational Option Pricing. *The Bell Journal of Economics and Management Science*, 4(1):141–183, 1973.

[5] Zvi Bodie, Alex Kane, and Alan Marcus. *Investments*. McGraw-Hill Irwin, 7 edition, 2008.

[6] Jim Gatheral. *The Volatility Surface: a Practitioner's Guide*. John Wiley & Sons, Inc., 2006.

[7] Riccardo Rebonato. *Volatility and Correlation in the Pricing of Equity, FX, and Interest Rate Options*. Wiley, 1999.

[8] Bruno Dupire. Pricing with a smile. *Risk*, 7:18–20, 1994.

[9] Emanual Derman and Iraj Kani. Riding on a smile. *Risk*, 7:32–39, 1994.

[10] RC Merton. Option pricing when underlying stock returns are discontinuous. *Journal of Financial Economics*, 3:125–144, 1976.

[11] Ioannis Karatzas and Steven E Shreve. *Methods of Mathematical Finance*, volume 39. Springer, 1998.

[12] Peter Carr and Liuren Wu. What Type of Process Underlies Options? A Simple Robust Test. *The Journal of Finance*, LVIII(6):2581–2610, 2003.

[13] Peter Carr and Dilip Madan. Option Valuation Using the Fast Fourier Transform. *Journal of Computational Finance*, pages 1–18, 1999.

[14] Alan L. Lewis. A Simple Option Formula for General Jump-Diffusion and Other Exponential Levy Processes. *Available at SSRN 282110*, 2001.

[15] Umberto Cherubini, Giovanni Della Lunga, Sabrina Mulinacci, and Pietro Rossi. *Fourier Transform Methods in Finance*. Wiley, 2010.

[16] Eugene Seneta and Dilip B. Madan. The Variance Gamma ( V . G .) Model for Share Market Returns. *The Journal of Business*, 63(4):511–524, 1990.

[17] Dilip B. Madan and Frank Milne. Option Pricing with V. G. Martingale Components. *Mathematical Finance*, 1(4):39–55, 1991.

[18] Dilip B. Madan, Peter Carr, and Eric C. Chang. The Variance Gamma Process and Option Pricing. *European Finance Review*, 2:79–105, 1998.

[19] Ole E Barndorff-Nielsen. Processes of Normal Inverse Gaussian Type. *Finance and Stochastics*, 68(September 1996):41–68, 1998.

[20] Ernst Eberlein and Ulrich Keller. Hyperbolic distributions in finance. *Bernoulli*, 1(3):281–299, 1995.

[21] Peter Carr, Hélyette Geman, Dilip B Madan, and Marc Yor. The Fine Structure of Asset Returns : An Empirical Investigation. *The Journal of Business*, 75(2):305–333, 2002.

[22] Svetlana I Boyarchenko and Sergei Z Levendorskii. *Non-Gaussian Merton-Black-Scholes Theory*. World Scientific, 2002.

[23] Wim Schoutens and Jozef L Teugels. Lévy processes, polynomials and martingales. *Stochastic Models*, 14(1-2):335–349, 1998.

[24] Alexey Kuznetsov. Wiener Hopf factorization and distribution of extrema for a family of Lévy processes. *The Annals of Applied Probability*, 20(5):1801–1830, October 2010.

[25] Alexey Kuznetsov, A. E. Kyprianou, J. C. Pardo, and K. van Schaik. A Wiener Hopf Monte Carlo simulation technique for Lévy processes. *The Annals of Applied Probability*, 21(6):2171–2190, December 2011.

[26] Wim Schoutens. *Lévy Processes in Finance*. Wiley, 2003.

[27] Rama Cont and José Da Fonseca. Dynamics of implied volatility surfaces. *Quantitative finance*, 2(1):45–60, 2002.

[28] Mikhail Konikov and Dilip B Madan. Option Pricing Using Variance Gamma Markov Chains. *Review of Derivatives Research*, 5:81–115, 2002.

[29] Gurdip Bakshi and Dilip B. Madan. Spanning and derivative-security valuation. *Journal of Financial Economics*, 55(October 1998):205–238, 2000.

[30] Peter Carr and Dilip B. Madan. Optimal Positioning in Derivative Securities. *Quantitative Finance*, 1(1):19–37, January 2001.

[31] Peter Carr, Helyette Geman, Dilip B. Madan, and Marc Yor. Self Decomposability and Option Pricing. *Mathematical finance*, pages 31–57, 2006.

[32] Dilip B. Madan, Helyette Geman, Marc Yor, and Peter Carr. Stochastic Volatility for Levy Processes. *Mathematical Finance*, 13:345–382, 2003.

[33] Rama Cont. Empirical Properties of Asset Returns: Stylized Facts and Statistical Issues. *Quantitative Finance*, 1(2):223–236, February 2001.

[34] John Hull and Alan White. The pricing of options on assets with stochastic volatilities. *The Journal of Finance*, XLII:281–300, 1987.

[35] Elias M. Stein and Jeremy C. Stein. Stock Price Distributions with Stochastic Volatility: An Analytic Approach. *Review of Financial Studies*, 4(4):727–752, October 1991.

[36] Steven L. Heston. A Closed-Form Solution for Options with Stochastic Volatility with Applications to Bond and Currency Options. *Review of Financial Studies*, 6:327–343, 1993.

[37] Eric Benhamou, Emmanuel Gobet, and Mohammed Miri. Time dependent heston model. *SIAM Journal on Financial Mathematics*, 1(1):289–325, 2010.

[38] David S. Bates. Jumps and stochastic volatility: Exchange rate processes implicit in Deutsche Mark options. *The Review of Financial Studies*, 9(1):69–107, 1996.

[39] Ole E. Barndorff-Nielsen and Neil Shephard. Econometric Analysis of Realized Volatility Models use in Estimating Stochastic Volatility Models. *Journal of the Royal Statistical Society: Series B (Statistical Methodology)*, 64(1):253–380, 2002.

[40] Mark H.A. Davis and David G. Hobson. The Range of Traded Option Prices. *Mathematical Finance*, 17:1–14, 2006.

[41] Dilip B. Madan. Stochastic Processes in Finance. *Annual Review of Financial Economics*, 2(1):277–314, December 2010.

[42] Ken-Iti Sato. *Lévy Processes and Infinitely Divisible Distributions*. Cambridge University Press, 1999.

[43] Andreas E. Kyprianou. *Introductory Lectures on Fluctuations of Lévy Processes with Applications*. Springer, 2006.

[44] Jean Bertoin. *Lévy Processes*. Cambridge University Press, 1996.

[45] J.F.C. Kingman. Completely random measures. *Pacific Journal of Mathematics*, 21(1):59–78, 1967.

[46] Erhan Cinlar. *Probability and Stochastics*. Springer, 2010.

[47] Elias M. Stein and Rami Shakarchi. *Real Analysis: Measure Theory, Integration, and Hilbert Spaces*. Princeton University Press, 2005.

[48] Walter Rudin. *Real and Complex Analysis, Third Edition*. McGraw–Hill, 1987.

[49] J.F.C. Kingman. *Poisson Processes*. Oxford University Press, 1993.

[50] Ioannis Karatzas and Steven E. Shreve. *Brownian Motion and Stochastic Calculus: Second Edition*. Springer, 1998.

[51] Robert B. Ash and Catherine A. Doléans-Dade. *Probability and Measure Theory: Second Edition*. Hardcourt Academic Press, 2000.

[52] Hiroshi Kunita and Shinzo Watanabe. On Square Integrable Martingales. *Nagoya Mathematical Journal*, 30:209–245, 1967.

[53] S. Bochner. Diffusion Equation and Stochastic Processes. *Proceedings of the National Academy of Sciences of the United States of America*, 35(7):368–370, 1949.

[54] S. Bochner. *Harmonic Analysis and the Theory of Probability*. University of California Press, 1955.

[55] Peter K. Clark. A Subordinated Stochastic Process Model with Finite Variance for Speculative Prices. *Econometrica*, 41(1):135–155, 1973.

[56] Hélyette Geman and Thierry Ané. Stochastic Subordination. *Risk*, 9:145–149, 1996.

[57] Ali Hirsa and Dilip B. Madan. Pricing American Options Under Variance Gamma. *Journal of Computational Finance*, 7:63–80, 2004.

[58] Patrick Fitzpatrick and Halsey Royden. *Real Analysis Fourth Edition*. Prentice Hall, 2010.

[59] Einar Hille. *Functional Analysis and Semi-Groups*. American Mathematical Society, 1948.

[60] Kôsaku Yosida. On the Differentiability and the Representation of One-Parameter Semi-Group of Linear Operators. *Journal of the Mathematical Society of Japan*, 1(1):15–21, 1948.

[61] Ken-Iti Sato. Cores Of Potential Operators for Processesses with Stationary Independent Increments. *Nagoya Mathematical Journal*, 48:129–146, 1972.

[62] Kiyoshi Itô. On stochastic differential equations. *Memoirs of the American Mathematical Society*, 4:1–51, 1951.

[63] G.A. Hunt. Semi-Groups of Measures on Lie Groups. *Transactions of the American Mathematical Society*, 81(2):264–293, 1956.

[64] Niels Jacob and René L. Schilling. Lévy-type processes and pseudo differential operators. *Lévy Processes: Theory and Applications, Birkhäuser, Boston*, pages 139–168, 2001.

[65] Jean Jacod and Albert Shiryaev. *Limit Theorems for Stochastic Processes*. Springer, second edition, 2003.

[66] Stewart N. Ethier and Thomas G. Kurtz. *Markov Processes: Characterization and Convergence*. Wiley, 1986.

[67] D.W. Stroock and S.R.S. Varadhan. Multidimensional diffusion processes, a series of comprehensive studies in mathematics, vol. 233, 1979.

[68] Daniel W. Stroock. Diffusion Processes Associated with Lévy generators. *Probability Theory and Related Fields*, 244:209–244, 1975.

[69] Richard F. Bass. Uniqueness in Law for Pure Jump Markov Processes. *Probability Theory and Related Fields*, 79:271–287, 1988.

[70] J. Michael Harrison and David M. Kreps. Martingales and Arbitrage in Multiperiod Securities Markets. *Journal of Economic Theory*, 408(20):381–408, 1979.

[71] J. Michael Harrison and Stanley R. Pliska. Martingales and Stochastic Integrals in the Theory of Continuous Trading. *Stochastic Processes and their Applications*, 11:215–260, 1981.

[72] J. Michael Harrison and Stanley R. Pliska. A Stochastic Calculus Model of Continuous Trading: Complete Markets. *Stochastic Processes and their Applications*, 15:313–316, 1983.

[73] F. Delbaen and W. Schachermayer. The Fundamental Theorem of Asset Pricing for Unbounded Stochastic Processes. *Mathematische Annalen*, 312:215–250, 1996.

[74] Al Shiryaev and Alexandar Cherny. Vector Stochastic Integrals and the Fundamental Theorem of Asset Pricing. *Proceedings of the Steklov Institute of Mathematics*, 2002.

[75] Y.M. Kabanov. Arbitrage theory. *Handbooks in Mathematical Finance: Option Pricing, Interest Rates and Risk Management, E. Jouini, J. Cvitaniśc and M. Musiela (Eds.)*, page 3, 2001.

[76] Aleksandar Mijatović and Martijn Pistorius. Continuously monitored barrier options under markov processes. *Mathematical Finance*, 2011.

[77] Stephen Figlewski and Bin Gao. The Adaptive Mesh Model : a New Approach to Efficient Option Pricing. *Journal of Financial Economics*, 53:313–351, 1999.

[78] Domingo Tavella and Curt Randall. *Pricing Financial Instruments: The Finite Difference Method*. Wiley, 2000.

[79] Nicholas J. Higham. The Scaling and Squaring Method for the Matrix Exponential Revisited. *SIAM Journal on Matrix Analysis and Applications*, 26(4):1179–1193, 2005.

[80] Rama Cont and Ekaterina Voltchkova. Integro-differential equations for option prices in exponential Lévy models. *Finance and Stochastics*, 9(3):299–325, July 2005.

[81] Aleksandar Mijatović and Martijn Pistorius. Continuously monitored barrier options under markov processes: Unabridged version with matlab code. Available at SSRN: http://ssrn.com/abstract-1462822, 2011.

[82] John C. Hull. *Options, Futures, and Other Derivatives*. Prentice Hall, eighth edition, 2011.

[83] Paul Glasserman. *Monte Carlo Methods in Financial Engineering*. Springer, 2004.

[84] Steven E. Shreve. *Stochastic Calculus for Finance*. Springer, 2004.

[85] Leif Andersen and Jesper Andreasen. Jump-Diffusion Processes: Volatility Smile Fitting and Numerical Methods for Option Pricing. *Review of Derivatives Research*, 4:231–262, 2000.

[86] Dilip B. Madan. S&P 500 Index Option Surface Drivers and their Real World and Risk Neutral Covariations (September 29, 2010). *Robert H. Smith School Research Paper No. RHS 06–130*, 2010.

[87] Rama Cont and Peter Tankov. *Financial Modelling with Jump Processes*. Chapman and Hal/CRC, 2004.

[88] J.A. Nelder and R. Mead. A Simplex Method for Function Minimization. *The Computer Journal*, 7:308–313, 1965.

[89] Jeffrey C. Lagarias, James A. Reeds, Margaret H. Wright, and Paul E. Wright. Convergence Properties of the Nelder–Mead Simplex Method in Low Dimensions. *SIAM Journal on Optimization*, 9(1):112–147, January 1998.

[90] Rama Cont and Peter Tankov. Calibration of Jump-Diffusion Option-Pricing Models : a Robust Non-Parametric Approach. *Journal of Computational Finance*, 7:1–49, 2003.

[91] V.M. Kruglov. A Note On Infinitely Divisible Distributions. *Theory of Probability & Its Applications*, 15(2):319–324, 1970.

[92] M. Plancherel and M. Leffler. Contribution à l'étude de la représentation dune fonction arbitraire par des intégrales définies. *Rendiconti del Circolo Matematico di Palermo (1884-1940)*, 30(1):289–335, 1910.

[93] M. Plancherel and M. Leffler. Sur la convergence et la sommabilité par les moyennes de $\lim_{x=\infty} \int_a^x f(x)cos(xy)dx$. *Mathematische Annalen*, 76:315–326, 1915.

[94] John J. Benedetto. *Harmonic Analysis and Applications*. CRC Press, 1997.

[95] Hélyette Geman. Pure jump Lévy processes for asset price modelling. *Journal of Banking & Finance*, 26(July):1297–1316, 2002.

[96] Michael T. Heideman, Don H. Johnson, and C. Sidney Burrus. Gauss and the History of the Fast Fourier Transform. *ASSP Magazine, IEEE*, pages 14–21, October 1984.

[97] James W. Cooley and John W. Tukey. An algorithm for the machine calculation of complex Fourier series. *Mathematics of Computation*, 19(90):297–301, 1965.